SUPPORTING INFORMATION

Halogen bonded cocrystals of active pharmaceutical ingredients: pyrazinamide, lidocaine and pentoxifylline in combination with haloperfluorinated compounds

Duane Choquesillo Lazarte*[a], Vinko Nemec,[b] and Dominik Cinčić*[b]

[a]Laboratorio de Estudios Cristalográficos, IACT (CSIC-UGR)
Avda. de las Palmeras 4, 18100 - Armilla (Granada), SPAIN
[b]Department of Chemistry, Faculty of Science, University of Zagreb,
Horvatovac 102a, HR-10000 Zagreb, Croatia

Email: dominik@chem.pmf.hr, duane.choquesillo@csic.es

Tel: +385 1 4606 362 (D.C.)
+34 958 230000 ext 190009 (D.C.L.)

Table of Contents

EXPERIMENTAL DETAILS

CSD SEARCH

The search was limited to datasets containing only organic fragments and the corresponding API fragment. Single component systems were manually removed from the resulting lists. In the **pza** search we obtained the following 29 datasets: **ASAYIC**, **EBONUC**; **EGENIP**, **HEDRAL**, **KIJSED**, **KOVSAR**, **KOVSEV**, **KOVSIZ**, **KOVSOF**, **LATTIL**, **LATTOR01**, **MUDVUE**, **NUFVEQ**, **NUSMIZ**, **NUVFIV**, **NUVFOB**, **PAQNOM**, **RACFIN**, **RACFIN01**, **REBXED**, **REBXIH**, **REBXON**, **REBXUT**, **SIHQOR**, **SIHRAE**, **URUGIY**, **VUTNAB** and **XAQQOW**. In the **ldc** search we obtained the following 9 datasets: **BENWUO**, **BIFJOR**, **DEWNOJ**, **LIDNPP**, **LIDOCA10**, **LIDOCN**, **LIDOCN01**, **ROYWIN**, **SEQRAJ**. In the **pxf** search we obtained the following 6 datasets: **FEFYAS**, **FEFYEW**, **FEFYIA**, **HUNJEH**, **HUNJIL**, **HUNJOR**.

MATERIALS

APIs, lidocaine (**ldc**) and pentoxifylline (**pxf**) were purchased from Fagron Ibérica and pyrazinamide (**pza**) was purchased from Sigma-Aldrich. Acetonitrile was purchased from J. T. Baker. Halogen bond donors, 1,4-diiodotetrafluorobenzene (**tfib)** and 1,4-dibromotetrafluorobenzene (**tfbb)** were purchased from Manchester Organics.

MECHANOCHEMICAL SYNTHESIS

Grinding of **pza** with **tfib** in a 1:1 stoichiometric ratio

pza (60.0 mg, 0.49 mmol) and **tfib** (195.9 mg, 0.49 mmol) were placed in a 10 mL stainless steel jar along with 10.0 μL of acetonitrile and two stainless steel balls 7 mm in diameter. The mixture was then milled for 20 minutes in a Retsch MM200 Shaker Mill operating at 25 Hz frequency.

Synthesis of (**pza**)$_2$(**tfib**)

pza (120.0 mg, 0.97 mmol) and **tfib** (195.9 mg, 0.49 mmol) were placed in a 10 mL stainless steel jar along with 10.0 μL of acetonitrile and two stainless steel balls 7 mm in diameter. The mixture was then milled for 20 minutes in a Retsch MM200 Shaker Mill operating at 25 Hz frequency.

Grinding of **pza** with **tfbb** in a 1:1 stoichiometric ratio

pza (75.0 mg, 0.61 mmol) and **tfbb** (187.6 mg, 0.61 mmol) were placed in a 10 mL stainless steel jar along with 10.0 μL of acetonitrile and two stainless steel balls 7 mm in diameter. The mixture was then milled for 20 minutes in a Retsch MM200 Shaker Mill operating at 25 Hz frequency.

Synthesis of (**pza**)$_2$(**tfbb**)

pza (150.0 mg, 1.22 mmol) and **tfbb** (187.6 mg, 0.61 mmol) were placed in a 10 mL stainless steel jar along with 10.0 μL of acetonitrile and two stainless steel balls 7 mm in diameter. The mixture was then milled for 20 minutes in a Retsch MM200 Shaker Mill operating at 25 Hz frequency.

Grinding of **ldc** with **tfib** in a 1:1 stoichiometric ratio

ldc (80.0 mg, 0.34 mmol) and **tfib** (137.2 mg, 0.34 mmol) were placed in a 10 mL stainless steel jar along with 10.0 μL of acetonitrile and two stainless steel balls 7 mm in diameter. The mixture was then milled for 20 minutes in a Retsch MM200 Shaker Mill operating at 25 Hz frequency.

Synthesis of (**ldc**)$_2$(**tfib**)

ldc (160.0 mg, 0.68 mmol) and **tfib** (137.2 mg, 0.34 mmol) were placed in a 10 mL stainless steel jar along with 10.0 μL of acetonitrile and two stainless steel balls 7 mm in diameter. The mixture was then milled for 20 minutes in a Retsch MM200 Shaker Mill operating at 25 Hz frequency.

Grinding of **ldc** with **tfbb** in a 1:1 stoichiometric ratio

ldc (80.0 mg, 0.34 mmol) and **tfbb** (105.1 mg, 0.34 mmol) were placed in a 10 mL stainless steel jar along with 10.0 μL of acetonitrile and two stainless steel balls 7 mm in diameter. The mixture was then milled for 20 minutes in a Retsch MM200 Shaker Mill operating at 25 Hz frequency.

Synthesis of (**ldc**)$_2$(**tfbb**)

ldc (160.0 mg, 0.68 mmol) and **tfbb** (105.1 mg, 0.34 mmol) were placed in a 10 mL stainless steel jar along with 10.0 μL of acetonitrile and two stainless steel balls 7 mm in diameter. The

mixture was then milled for 20 minutes in a Retsch MM200 Shaker Mill operating at 25 Hz frequency.

Synthesis of (**pxf**)(**tfib**)

pxf (40.0 mg, 0.14 mmol) and **tfib** (57.8 mg, 0.14 mmol) were placed in a 10 mL stainless steel jar along with 10.0 μL of acetonitrile and two stainless steel balls 7 mm in diameter. The mixture was then milled for 15 minutes in a Retsch MM200 Shaker Mill operating at 25 Hz frequency.

Grinding of **pxf** with **tfib** in a 2:1 stoichiometric ratio

pxf (80.0 mg, 0.28 mmol) and **tfib** (57.8 mg, 0.14 mmol) were placed in a 10 mL stainless steel jar along with 10.0 μL of acetonitrile and two stainless steel balls 7 mm in diameter. The mixture was then milled for 15 minutes in a Retsch MM200 Shaker Mill operating at 25 Hz frequency.

Grinding of **pxf** with **tfbb** in a 1:1 stoichiometric ratio

pxf (100.0 mg, 0.36 mmol) and **tfbb** (110.6 mg, 0.36 mmol) were placed in a 10 mL stainless steel jar along with 10.0 μL of acetonitrile and two stainless steel balls 7 mm in diameter. The mixture was then milled for 20 minutes in a Retsch MM200 Shaker Mill operating at 25 Hz frequency.

Synthesis of (**pxf**)$_2$(**tfbb**)

pxf (200.0 mg, 0.72 mmol) and **tfbb** (110.6 mg, 0.36 mmol) were placed in a 10 mL stainless steel jar along with 10.0 μL of acetonitrile and two stainless steel balls 7 mm in diameter. The mixture was then milled for 20 minutes in a Retsch MM200 Shaker Mill operating at 25 Hz frequency.

Preparation of single crystals

Single crystals were grown by solvent evaporation at room temperature using the polycrystalline material obtained from mechanical synthesis. Suitable crystals for X-ray diffraction studies were obtained from recrystallization in saturated solutions: dichloromethane [(**pza**)$_2$(**tfib**), (**pxf**)$_2$(**tfbb**)], acetonitrile [(**pza**)$_2$(**tfbb**)], ethanol [(**ldc**)$_2$(**tfib**), (**ldc**)$_2$(**tfbb**)] and tetrahydropyrane [(**pxf**)(**tfib**)].

THERMAL ANALYSIS

DSC of halogen bond donors were conducted using a Mettler-Toledo DSC823e module. The samples were placed into aluminium pans, and heated in flowing nitrogen (150 mL/min) from 25 °C to 500 °C at a rate of 10 °C/min.

DSC of API's and cocrystals were conducted using a Shimadzu DSC-50Q which was calibrated for temperature and enthalpy using indium. Samples (3-5 mg) were placed into aluminum pans. The thermograms were recorded by heating the samples from 25 to 200 °C at a rate of 10°C/min under nitrogen flow of 100 ml/min.

TGA was performed on a Mettler Toledo TGA 851 instrument. Approximately 5 mg sample was heated from 25 to 500 °C in open alumina pan at the rate of 10 °C/min under nitrogen purge at flow rate of 100 mL/min.

SINGLE-CRYSTAL X-RAY DIFFRACTION EXPERIMENTS

Measured crystals were prepared under inert conditions immersed in perfluoropolyether as protecting oil for manipulation. Suitable crystals were mounted on MiTeGen Micromounts™ and these samples were used for data collection. Data were collected with a Bruker D8 Venture diffractometer. The data were processed with APEX3 suite[1]. The structures were solved by direct methods[2], which revealed the position of all non-hydrogen atoms. These atoms were refined on F^2 by a full-matrix least-squares procedure using anisotropic displacement parameters[2]. All hydrogen atoms were located in difference Fourier maps and included as fixed contributions riding on attached atoms with isotropic thermal displacement parameters 1.2 times those of the respective atom. Crystallographic data for the structures of compounds in this paper have been deposited with the Cambridge Crystallographic Data Center as supplementary publication no. 1550372 [(**pza**)$_2$(**tfib**)], 1550373 [(**pza**)$_2$(**tfbb**)], 1550374 [(**ldc**)$_2$(**tfib**)], 1550375 [(**ldc**)$_2$(**tfbb**)], 1550376 [(**pxf**)(**tfib**)] and 1550377 [(**pxf**)$_2$(**tfbb**)]. Geometric calculations and molecular graphics were performed with Mercury[3] and Olex2[4]. Additional crystal data are shown in Tables S1-S3. Copies of the data can be obtained free of charge at http://www.ccdc.cam.ac.uk/products/csd/request/.

POWDER X-RAY DIFFRACTION EXPERIMENTS

PXRD experiments on the samples were performed on a PHILIPS PW 1840 X-ray diffractometer with CuKα_1 (1.54056 Å) radiation at 40 mA and 40 kV. The scattered intensities were measured with a scintillation counter. The angular range was from 5 to 40° (2θ) with a continuous step size of 0.03°, and measuring time of 0.3 s per step. Data collection and analysis was performed using the program package Philips X'Pert.[5]

References

1. Bruker, APEX3 Software, Bruker AXS Inc. V2016.1, Madison, Wisconsin, USA, (2016).

2. G.M. Sheldrick, Acta Crystallogr. A64 (2008) 112.

3. C.F. Macrae, I.J. Bruno, J.A. Chisholm, P.R. Edgington, P. McCabe, E. Pidcock, L. Rodriguez-Monge, R. Taylor, J. van de Streek, P.A. Wood, J. Appl. Crystallogr. 41 (2008) 466.

4. O.V. Dolomanov, L.J. Bourhis, R.J. Gildea, J.A.K. Howard, H. Puschmann, J. Appl. Crystallogr. 42 (2009) 339.

5. Philips X'Pert Data Collector 1.3e, Philips Analytical B. V. Netherlands, 2001; Philips X'Pert Graphic & Identify 1.3e Philips Analytical B. V. Netherlands, 2001; Philips X'Pert Plus 1.0, Philips Analytical B. V. Netherlands, 1999.

Table S1. General and crystallographic data for the prepared **pza** cocrystals.

	(pza)$_2$(tfib)	**(pza)$_2$(tfbb)**
Molecular formula	$C_{16}H_{10}F_4I_2N_6O_2$	$C_{16}H_{10}Br_2F_4N_6O_2$
M_r	648.10	554.12
Crystal system	Triclinic	Triclinic
Space group	*P*-1	*P*-1
Crystal data:		
a / Å	5.6157(3)	5.2164(8)
b / Å	5.8013(3)	5.7379(10)
c / Å	15.5403(8)	16.463(3)
α / °	85.616(2)	98.285(5)
β / °	89.138(2)	90.049(5)
γ / °	80.700(2)	102.844(5)
V / Å^3	498.16(5)	475.15(14)
Z	1	1
D_{calc} / g cm^{-3}	2.160	1.937
λ / Å	0.71073	0.71073
T / K	293(2)	293(2)
Crystal size / mm^3	0.12 x 0.1 x 0.1	0.14 x 0.1 x 0.1
μ / mm^{-1}	3.220	4.331
$F(000)$	306	270
Refl. collected/unique	8448/2295	8182/2091
Data/restraints/parameters	2295 / 0 / 136	2091 / 0 / 136
$\Delta\rho_{max}$, $\Delta\rho_{min}$ / e Å^{-3}	0.571 and -0.682	0.523 and -0.920
$R[F^2>4\sigma(F^2)]$	0.0278	0.0440
$wR(F^2)$	0.0593	0.0893
Goodness-of-fit, S	1.109	1.038

Table S2. General and crystallographic data for the prepared **ldc** cocrystals.

	(ldc)$_2$(tfib)	**(ldc)$_2$(tfbb)**
Molecular formula	$C_{17}H_{22}F_2IN_2O$	$C_{17}H_{22}BrF_2N_2O$
M_r	435.26	388.27
Crystal system	Monoclinic	Monoclinic
Space group	$P2_1/n$	$P2_1/n$
Crystal data:		
a / Å	8.3275(15)	8.1092(4)
b / Å	15.183(3)	14.9953(7)
c / Å	15.170(3)	15.2066(8)
α / °	90	90
β / °	100.678(6)	101.158(2)
γ / °	90	90
V / Å^3	1884.8(6)	1814.17(16)
Z	4	4
D_{calc} / g cm^{-3}	1.534	1.422
λ / Å	1.54178	0.71073
T / K	293(2)	293(2)
Crystal size / mm^3	0.14 x 0.12 x 0.1	0.14 x 0.12 x 0.12
μ / mm^{-1}	13.559	2.290
$F(000)$	868	796
Refl. collected/unique	15877/3308	21997/3686
Data/restraints/parameters	3308 / 0 / 213	3686 / 6 / 213
$\Delta\rho_{max}$, $\Delta\rho_{min}$ / e Å^{-3}	0.562 and -0.711	0.606 and -0.525
$R[F^2>4\sigma(F^2)]$	0.0449	0.0541
$wR(F^2)$	0.1228	0.1453
Goodness-of-fit, S	1.070	1.057

Table S3. General and crystallographic data for the prepared **pxf** cocrystals.

	(pxf)(tfib)	**(pxf)$_2$(tfbb)**
Molecular formula	$C_{19}H_{18}F_4I_2N_4O_3$	$C_{32}H_{36}Br_2F_4N_8O_6$
M_r	680.17	864.51
Crystal system	Orthorhombic	Triclinic
Space group	*P*na2$_1$	*P*-1
Crystal data:		
a / Å	16.5437(5)	5.0832(6)
b / Å	31.4061(9)	11.3132(14)
c / Å	4.48440(10)	16.794(2)
α / °	90	107.353(7)
β / °	90	96.484(7)
γ / °	90	90.132(7)
V / Å^3	2329.97(11)	915.3(2)
Z	4	1
D_{calc} / g cm^{-3}	1.939	1.568
λ / Å	1.54178	1.54178
T / K	293(2)	293(2)
Crystal size / mm^3	0.10 x 0.10 x 0.08	0.11 x 0.08 x 0.08
μ / mm^{-1}	21.754	3.463
F(*000*)	1304	438
Refl. collected/unique	39935/4107	13571/3221
Data/restraints/parameters	4107 / 1 / 293	3221 / 0 / 239
$\Delta\rho_{max}$, $\Delta\rho_{min}$ / e Å^{-3}	0.835 and -0.552	0.378 and -0.395
$R[F^2>4\sigma(F^2)]$	0.0531	0.0510
$wR(F^2)$	0.1338	0.1236
Goodness-of-fit, *S*	1.031	1.049

Table S4. Geometric parameters for the halogen bonds in prepared cocrystals. Distances between select atoms in a contact are denoted as *d*, while the corresponding angle is marked with α.

Compound	***D***-X···***A***	*d*(**D**-X) / Å	*d*(**X**···**A**) / Å	α/°	**Symmetry operator**
(**pza**)$_2$(**tfib**)	C6-I1···N3	2.090(3)	3.044	175.245	--
(**pza**)$_2$(**tfbb**)	C6-Br1···N3	1.875(4)	3.092	179.494	--
(**ldc**)$_2$(**tfib**)	C15-I1···O1	2.086(5)	2.926	170.289	--
(**ldc**)$_2$(**tfbb**)	C15-Br1···O1	1.880(4)	3.101	169.859	--
(**pxf**)(**tfib**)	C14-I1···O3	2.072(16)	2.934	169.997	*x, y, 1+z*
	C17-I2···N3	2.102(15)	2.949	172.205	*1/2-x, -1/2+y, -1/2+z*
(**pxf**)$_2$(**tfbb**)	C14-Br1···O2	1.862(5)	2.821	173.649	--

Table S5. Geometric parameters for the hydrogen bonds in prepared cocrystals. Distances between select atoms in a contact are denoted as *d*, while the corresponding angle is marked with α.

Compound	***D***-H···***A***	*d*(***D***-H) / Å	*d*(H···**A**) / Å	*d*(***D***-H···***A***) / Å	***α***/°	**Symmetry operator**
(pza)$_2$(tfib)	N1-H1A···O1	0.86	2.06	2.916(4)	177.3	*3-x, 1-y, -z*
	N1-H1B···N2	0.86	2.32	2.691(5)	106	--
(pza)$_2$(tfbb)	N1-H1A···O1	0.86	2.05	2.904(4)	174.1	*3-x, 1-y, -z*
	N1-H1B···N2	0.86	2.34	2.705(5)	106	--
(ldc)$_2$(tfib)	N1-H1···N2	0.86	2.25	2.697(6)	111.9	
(ldc)$_2$(tfbb)	N1-H1···N2	0.86	2.25	2.694(4)	112.4	
(pxf)(tfib)	C2-H2B···O1	0.97	2.56	3.12(3)	117	
	C8-H8A···O2	0.96	2.32	2.75(3)	106	
	C12-H12···O1	0.93	2.34	3.26(3)	168	*1/2+x,3/2-y,1+z*
(pxf)$_2$(tfbb)	C1-H1B···O3	0.97	2.34	2.726(6)	103	
	C4-H4B···O1	0.97	2.52	3.446(7)	161	*1+x,y,z*
	C8-H8C···N3	0.96	2,47	2.914(8)	108	
	C12-H12···N3	0.93	2.43	3.258(7)	148	*3-x,2-y,1-z*
	C13-H13C···O3	0.96	2.55	3.494(7)	169	*2-x,1-y,1-z*

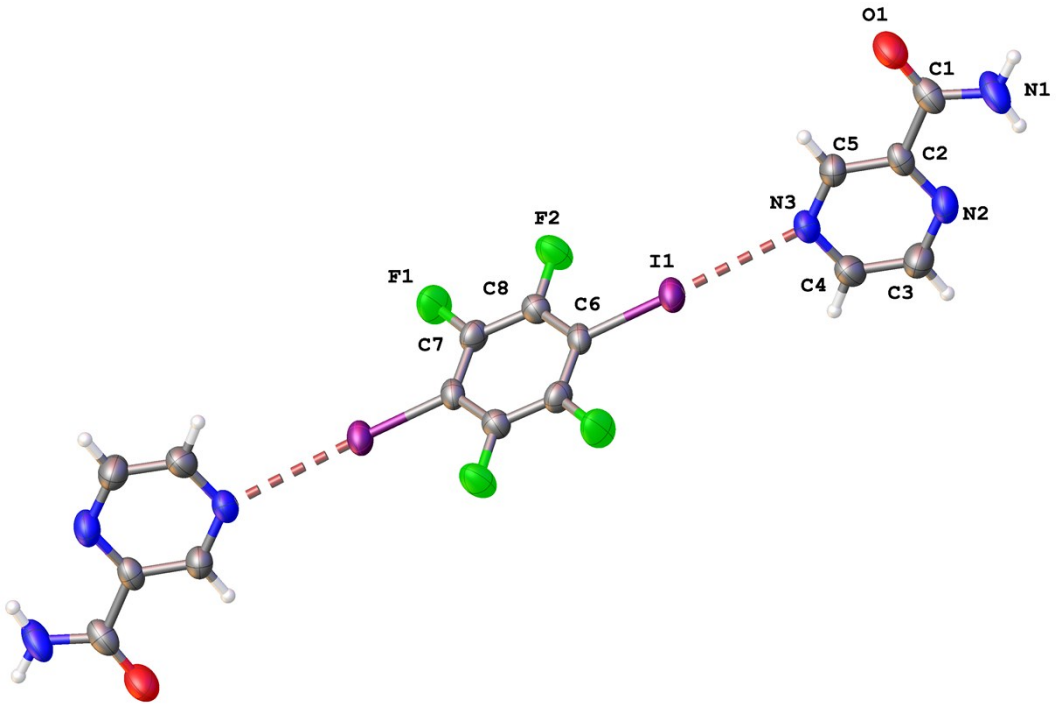

Figure S1. Molecular structure of (**pza**)$_2$(**tfib**) showing the atom-labelling scheme. Displacement ellipsoids are drawn at the 50 % probability level, halogen bonds are marked with red dashed lines, and H atoms are shown as small spheres of arbitrary radius.

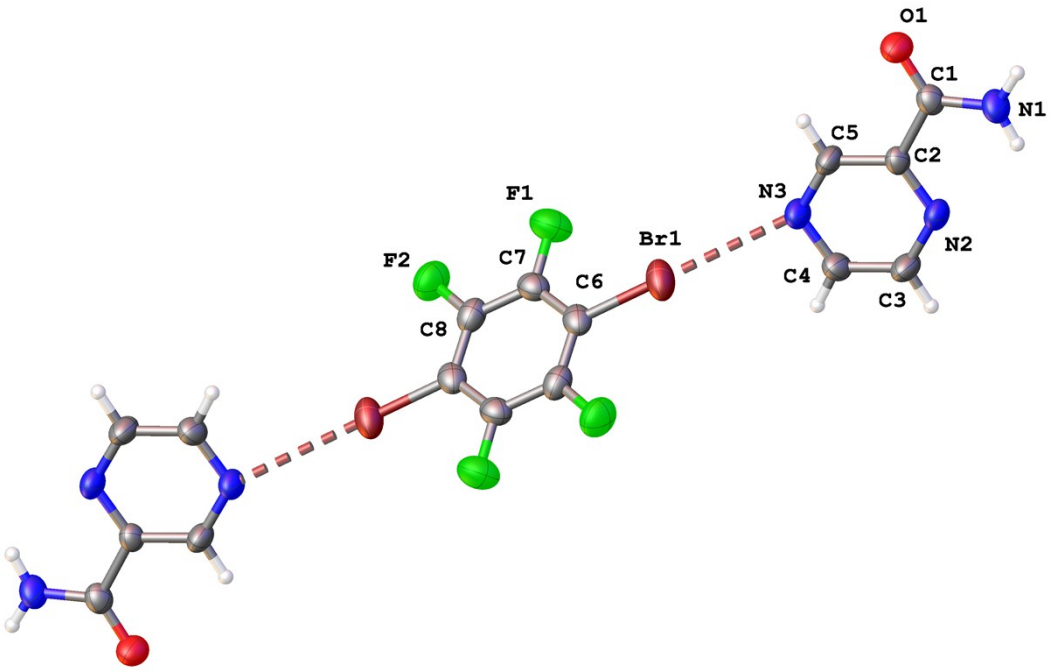

Figure S2. Molecular structure of (**pza**)$_2$(**tfbb**) showing the atom-labelling scheme. Displacement ellipsoids are drawn at the 50 % probability level, halogen bonds are marked with red dashed lines, and H atoms are shown as small spheres of arbitrary radius.

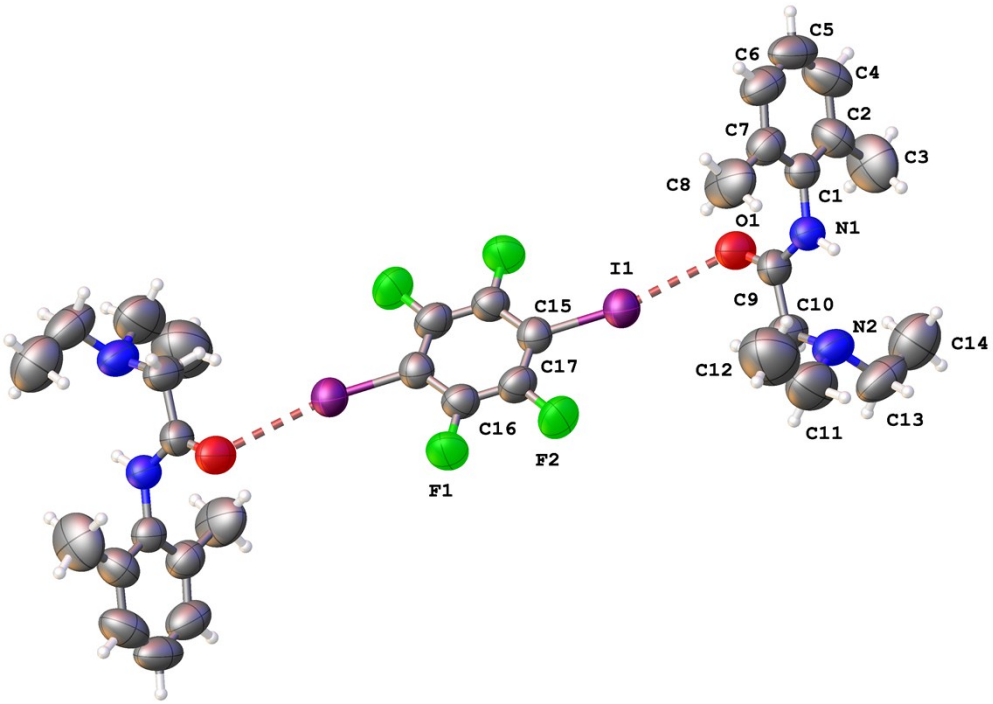

Figure S3. Molecular structure of (**ldc**)$_2$(**tfib**) showing the atom-labelling scheme. Displacement ellipsoids are drawn at the 50 % probability level, halogen bonds are marked with red dashed lines, and H atoms are shown as small spheres of arbitrary radius.

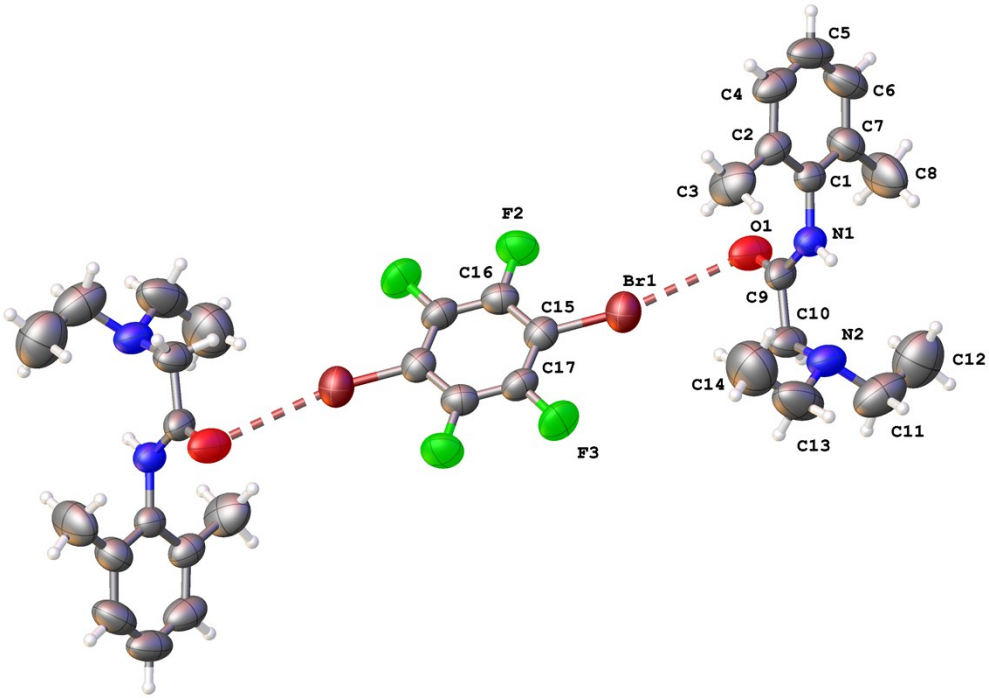

Figure S4. Molecular structure of (**ldc**)$_2$(**tfbb**) showing the atom-labelling scheme. Displacement ellipsoids are drawn at the 50 % probability level, halogen bonds are marked with red dashed lines, and H atoms are shown as small spheres of arbitrary radius.

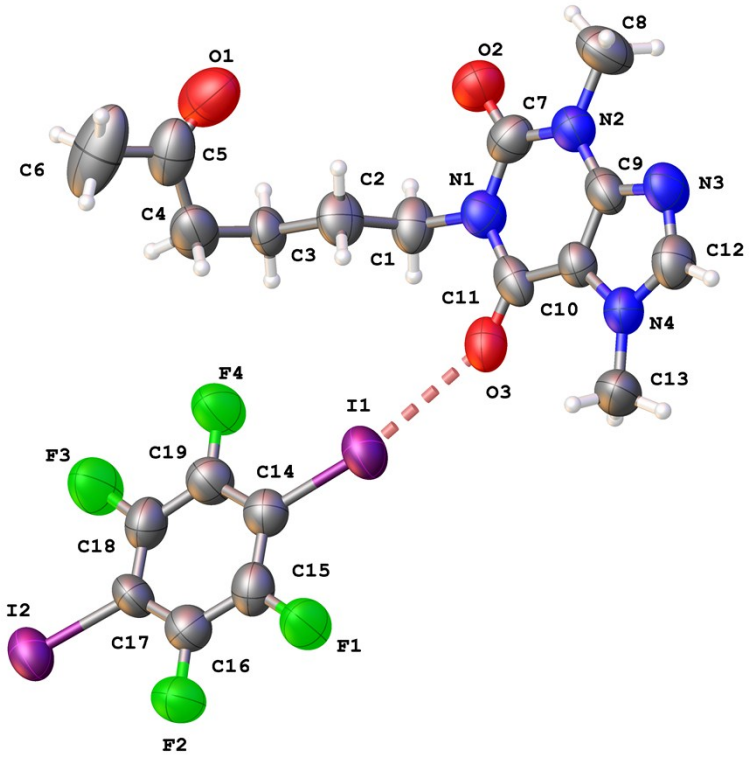

Figure S5. Molecular structure of (**pxf**)(**tfib**) showing the atom-labelling scheme. Displacement ellipsoids are drawn at the 50 % probability level, halogen bonds are marked with red dashed lines, and H atoms are shown as small spheres of arbitrary radius.

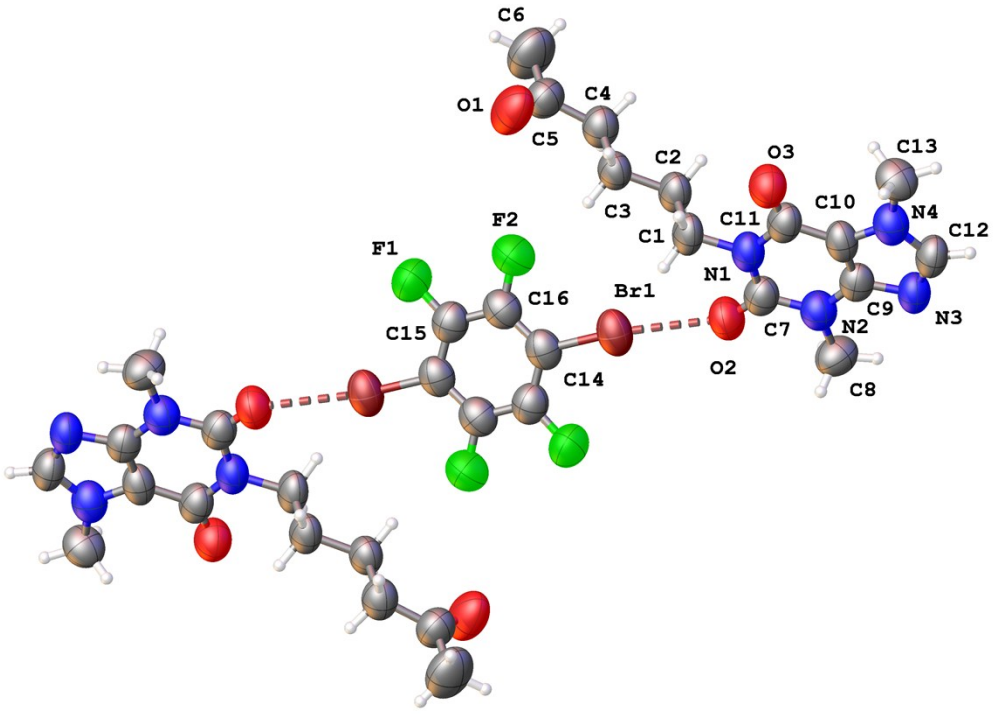

Figure S6. Molecular structure of (**pxf**)$_2$(**tfbb**) showing the atom-labelling scheme. Displacement ellipsoids are drawn at the 50 % probability level, halogen bonds are marked with red dashed lines, and H atoms are shown as small spheres of arbitrary radius.

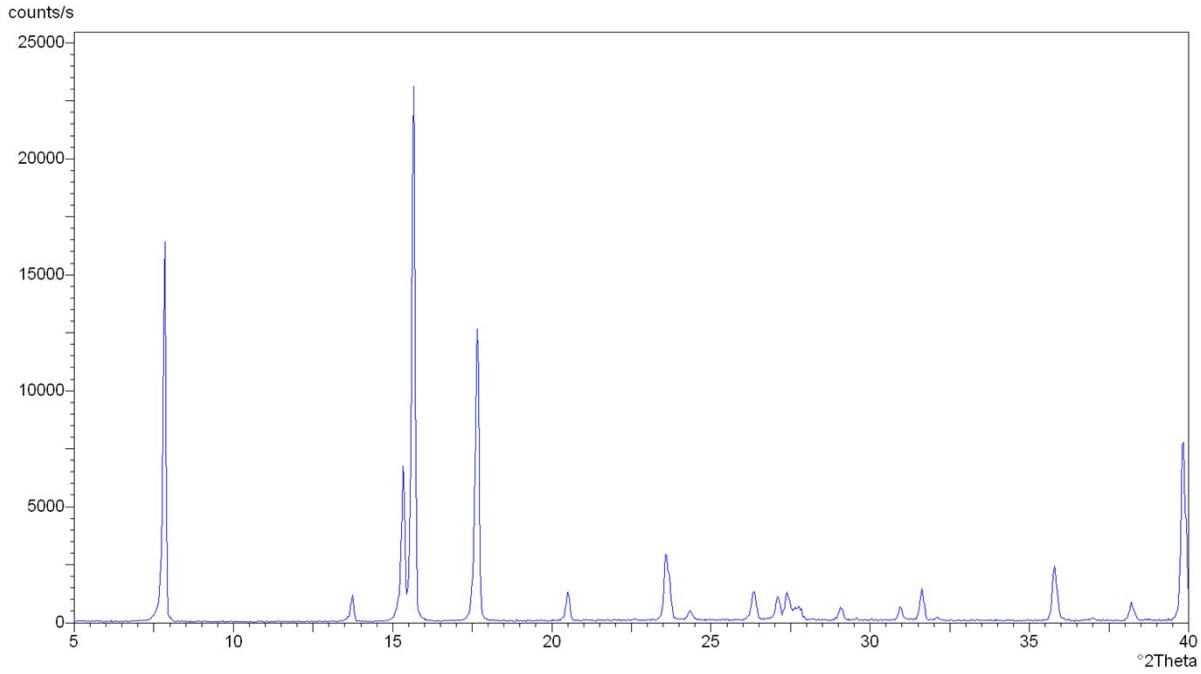

Figure S7. PXRD pattern of pure **pza** reactant.

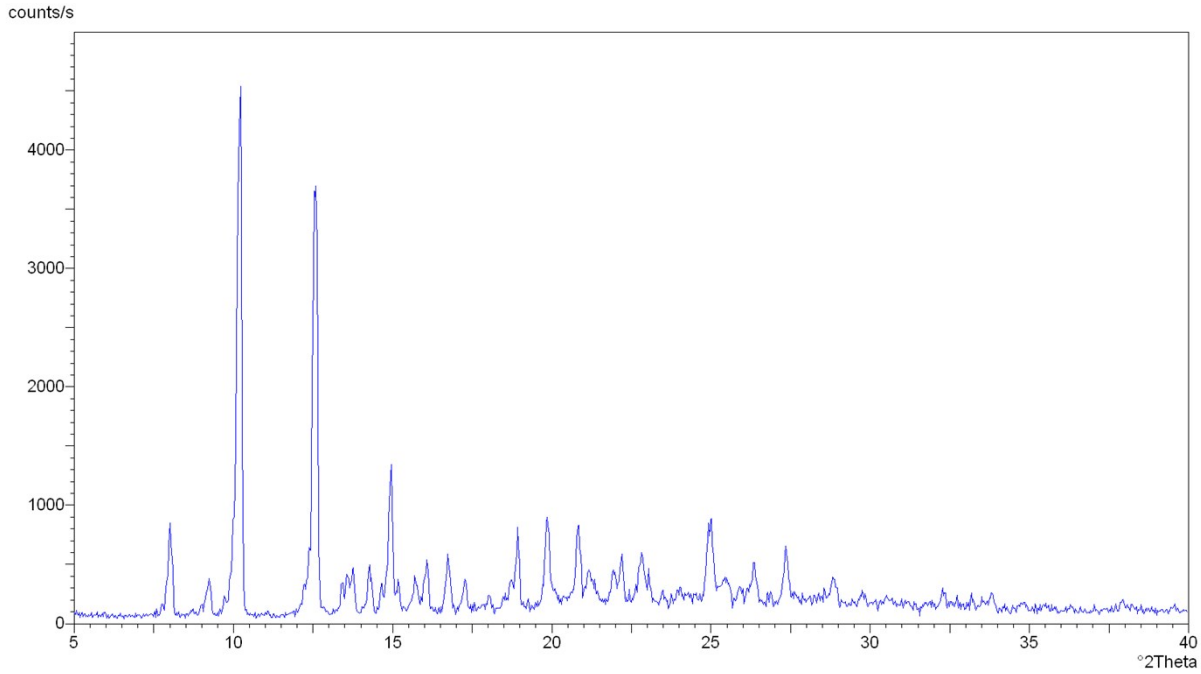

Figure S8. PXRD pattern of pure **ldc** reactant.

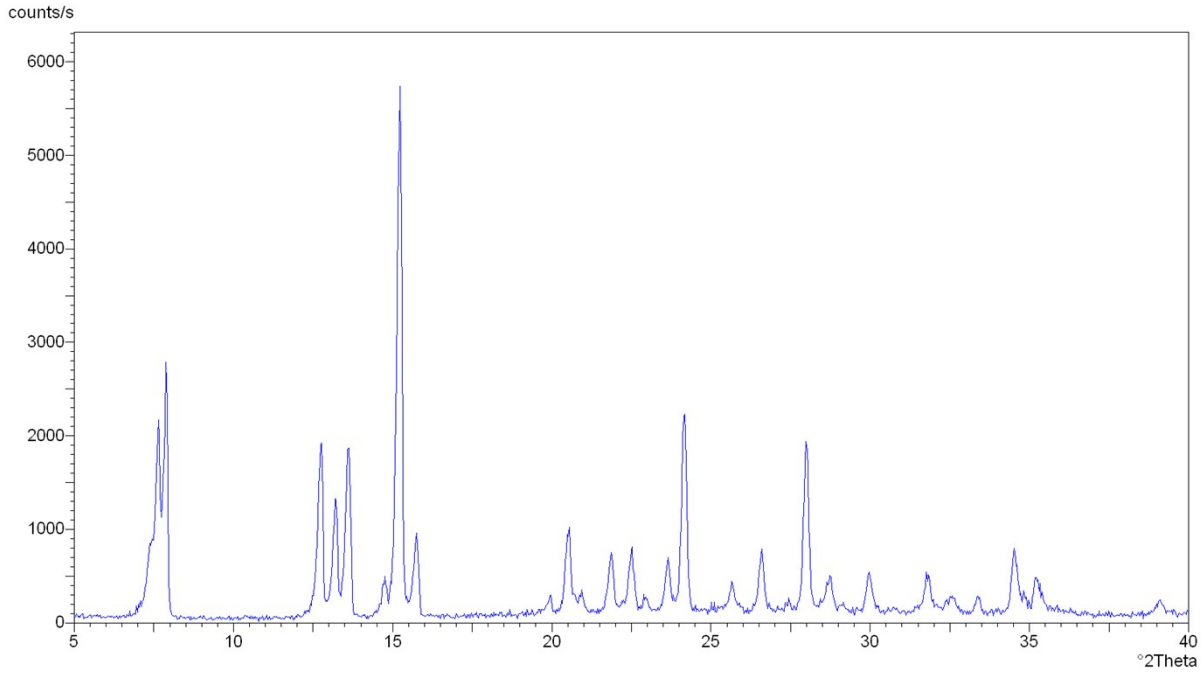

Figure S9. PXRD pattern of pure **pxf** reactant.

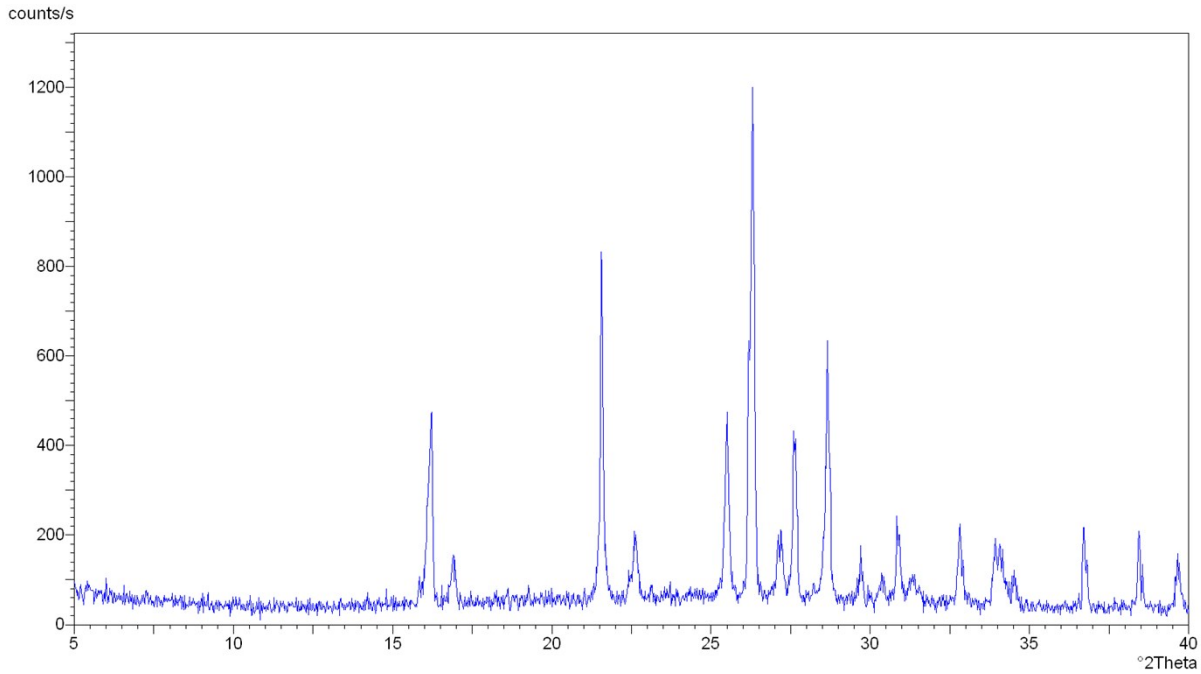

Figure S10. PXRD pattern of pure **tfib** reactant.

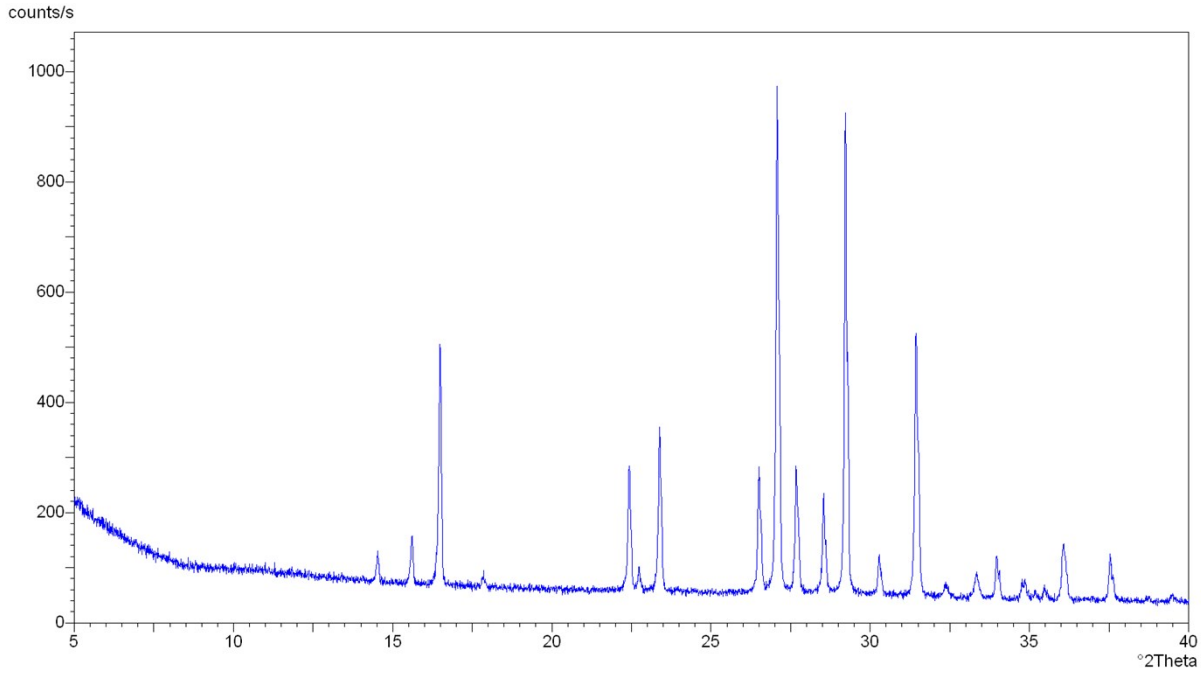

Figure S11. PXRD pattern of pure **tfbb** reactant.

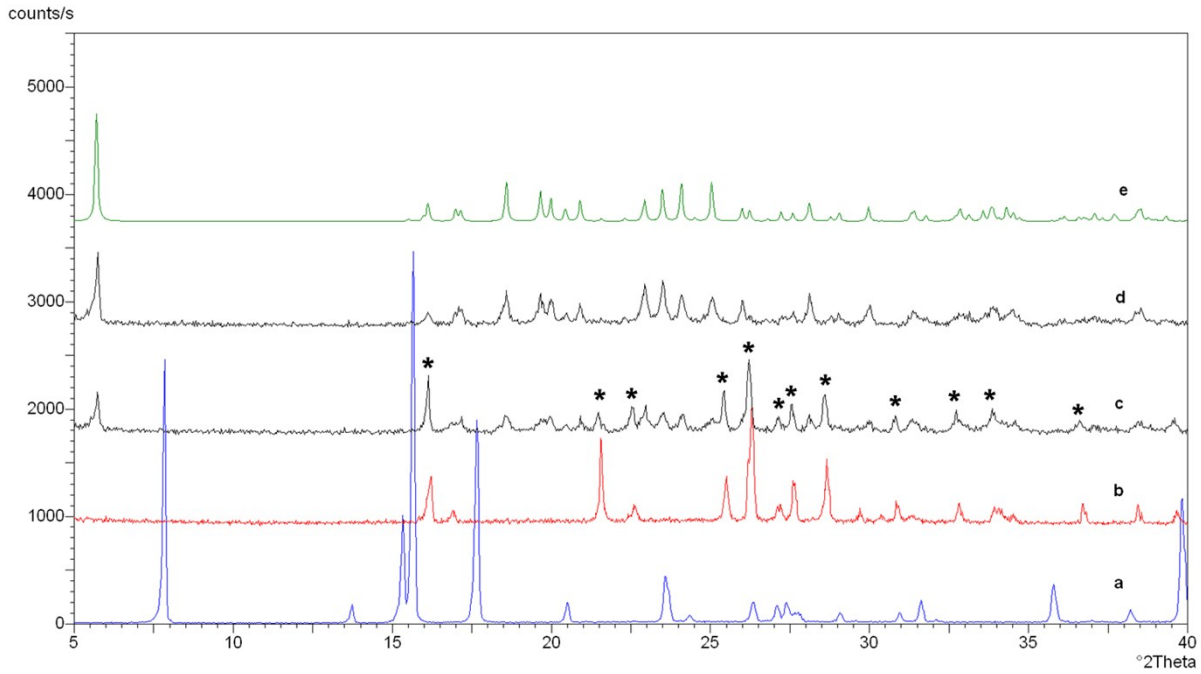

Figure S12. PXRD patterns of: a) **pza**, b) **tfib**, c) product obtained by grinding a mixture with a 1:1 molar ratio of **pza** to **tfib** in a ball mill for 20 min in the presence of 10 μL of acetonitrile (***** = diffraction maxima corresponding to surplus **tfib**), d) product obtained by grinding a mixture with a 2:1 molar ratio of **pza** to **tfib** in a ball mill for 20 min in the presence of 10 μL of acetonitrile, e) calculated pattern for (**pza**)$_2$(**tfib**).

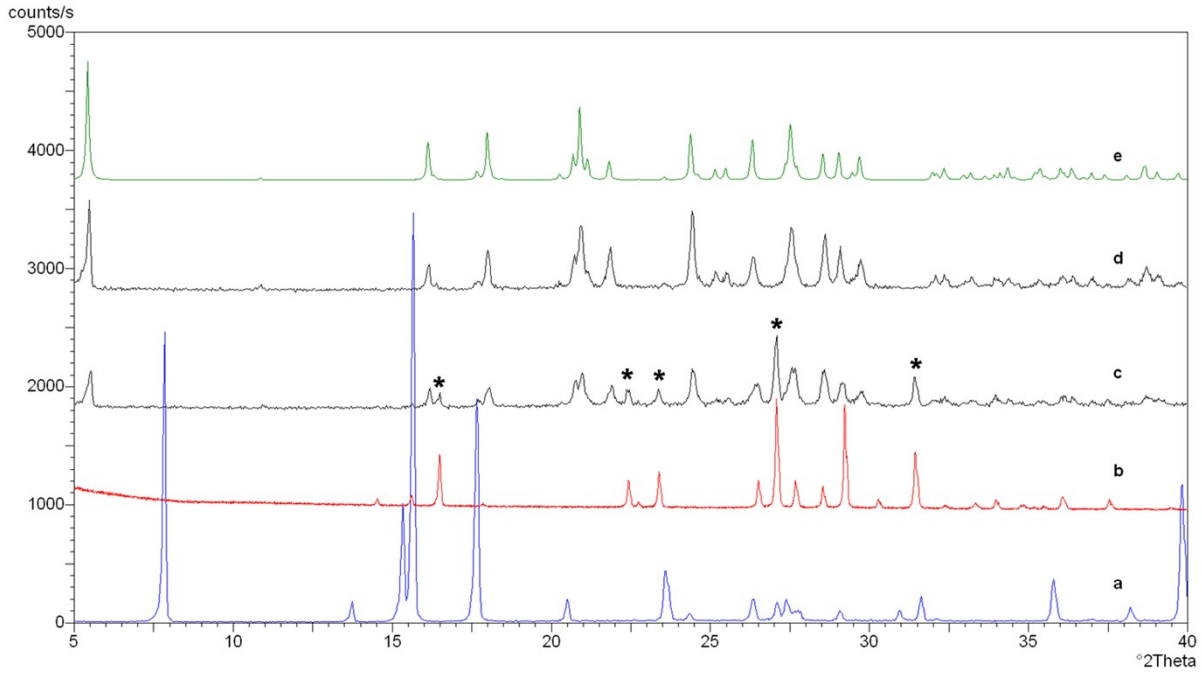

Figure S13. PXRD patterns of: a) **pza**, b) **tfbb**, c) product obtained by grinding a mixture with a 1:1 molar ratio of **pza** to **tfbb** in a ball mill for 20 min in the presence of 10 μL of acetonitrile (***** = diffraction maxima corresponding to surplus **tfbb**), d) product obtained by grinding a mixture with a 2:1 molar ratio of **pza** to **tfbb** in a ball mill for 20 min in the presence of 10 μL of acetonitrile, e) calculated pattern for (**pza**)$_2$(**tfbb**).

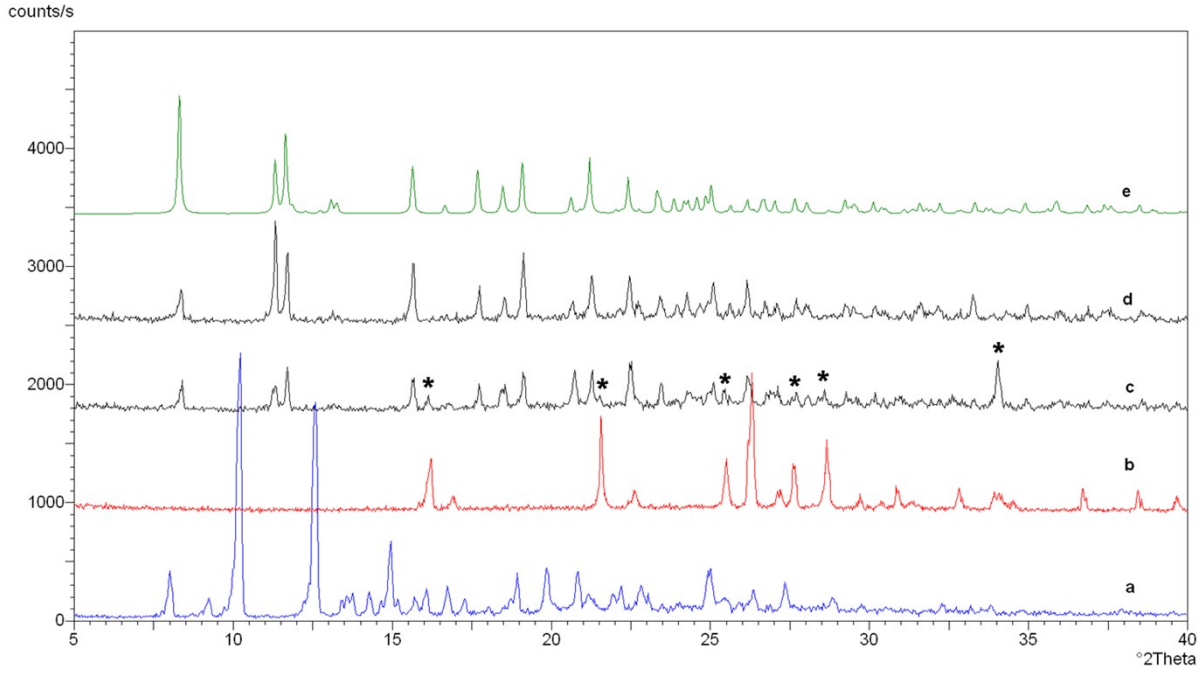

Figure S14. PXRD patterns of: a) **ldc**, b) **tfib**, c) product obtained by grinding a mixture with a 1:1 molar ratio of **ldc** to **tfib** in a ball mill for 20 min in the presence of 10 μL of acetonitrile (***** = diffraction maxima corresponding to surplus **tfib**), d) product obtained by grinding a mixture with a 2:1 molar ratio of **ldc** to **tfib** in a ball mill for 20 min in the presence of 10 μL of acetonitrile, e) calculated pattern for (**ldc**)$_2$(**tfib**).

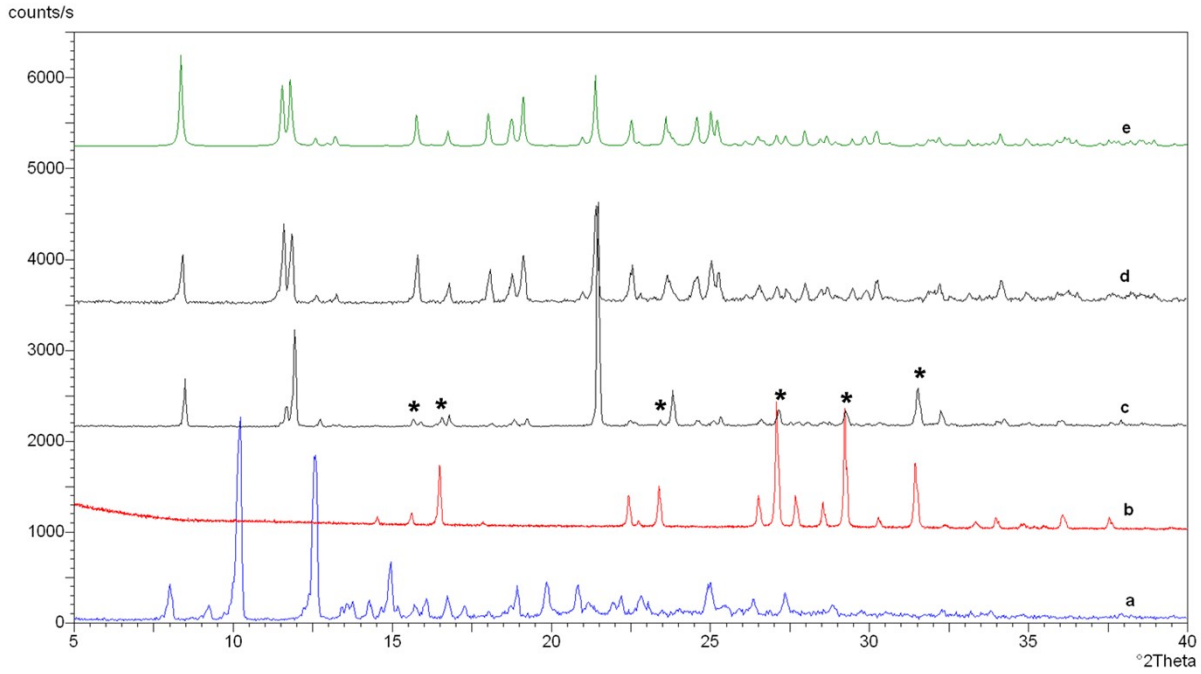

Figure S15. PXRD patterns of: a) **ldc**, b) **tfbb**, c) product obtained by grinding a mixture with a 1:1 molar ratio of **ldc** to **tfbb** in a ball mill for 20 min in the presence of 10 μL of acetonitrile (***** = diffraction maxima corresponding to surplus **tfbb**), d) product obtained by grinding a mixture with a 2:1 molar ratio of **ldc** to **tfbb** in a ball mill for 20 min in the presence of 10 μL of acetonitrile, e) calculated pattern for (**ldc**)$_2$(**tfbb**).

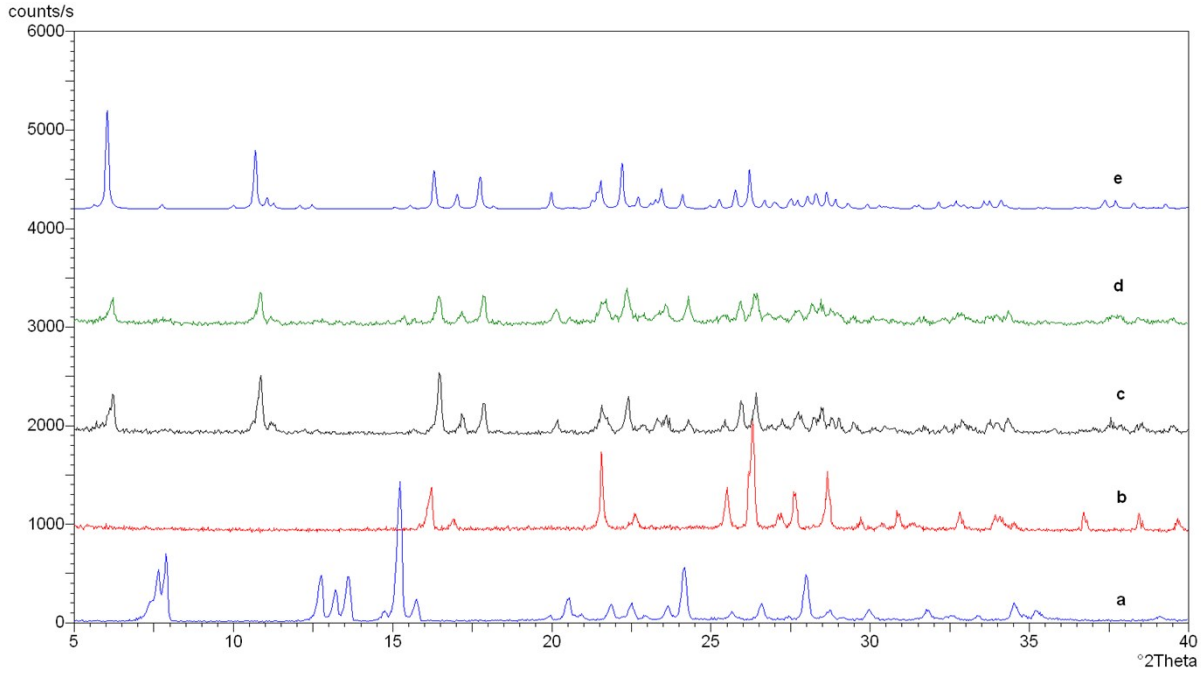

Figure S16. PXRD patterns of: a) **pxf**, b) **tfib**, c) product obtained by grinding a mixture with a 1:1 molar ratio of **pxf** to **tfib** in a ball mill for 20 min in the presence of 10 μL of acetonitrile, d) product obtained by grinding a mixture with a 2:1 molar ratio of **pxf** to **tfib** in a ball mill for 20 min in the presence of 10 μL of acetonitrile, e) calculated pattern for (**pxf**)(**tfib**).

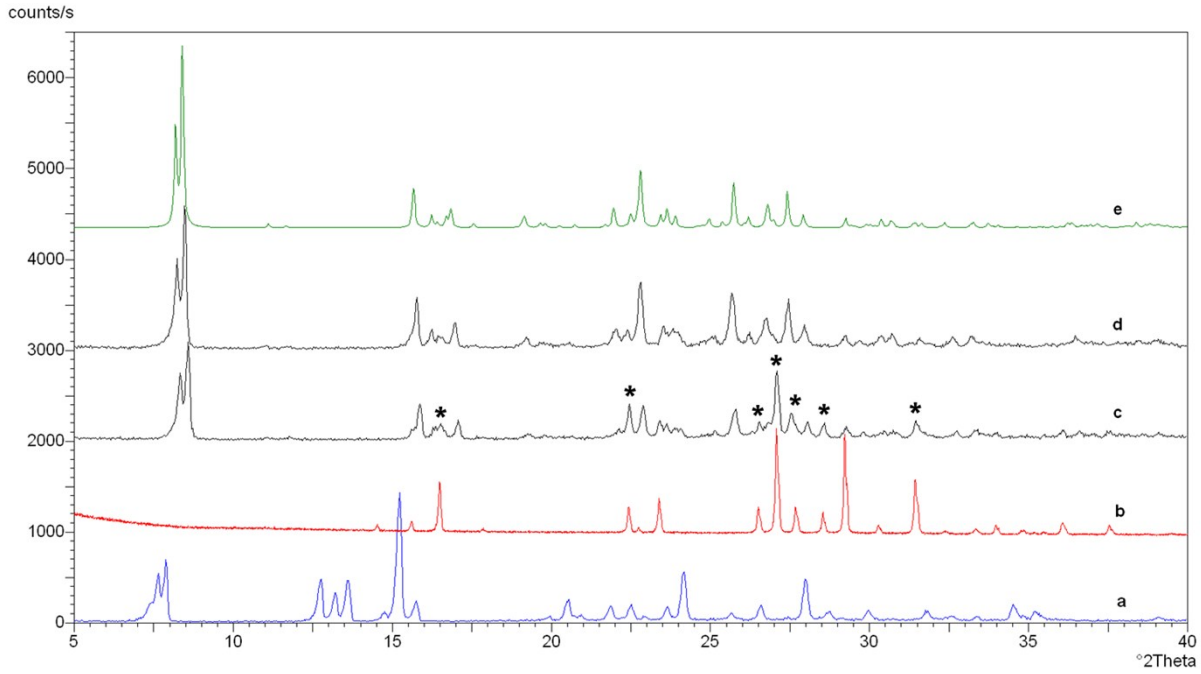

Figure S17. PXRD patterns of: a) **pxf**, b) **tfbb**, c) product obtained by grinding a mixture with a 1:1 molar ratio of **pxf** to **tfbb** in a ball mill for 20 min in the presence of 10 μL of acetonitrile (***** = diffraction maxima corresponding to surplus **tfbb**), d) product obtained by grinding a mixture with a 2:1 molar ratio of **pxf** to **tfbb** in a ball mill for 20 min in the presence of 10 μL of acetonitrile, e) calculated pattern for (**pxf**)$_2$(**tfbb**).

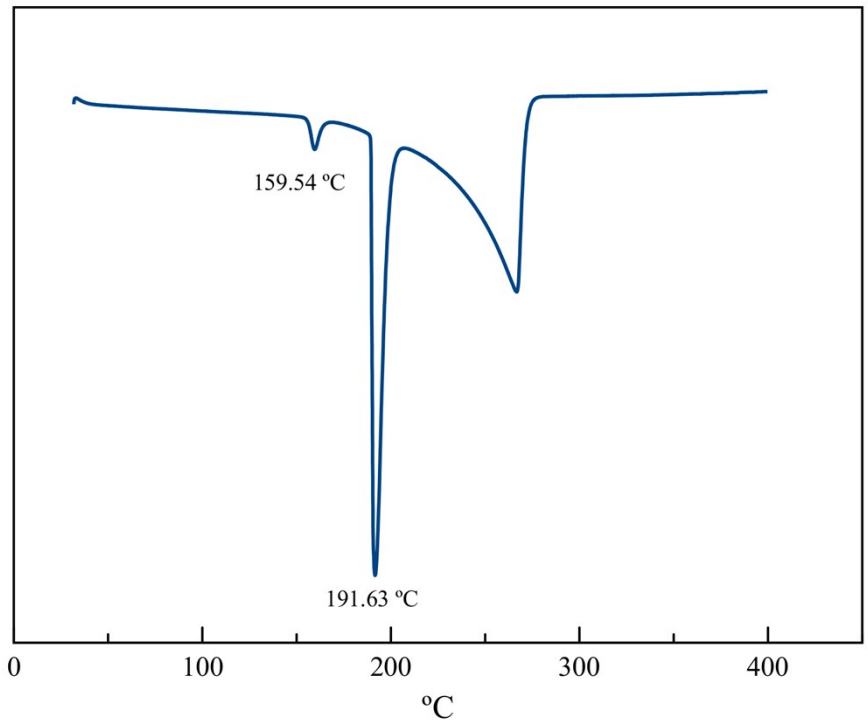

Figure S18. DSC curve of the pure **pza** reactant.

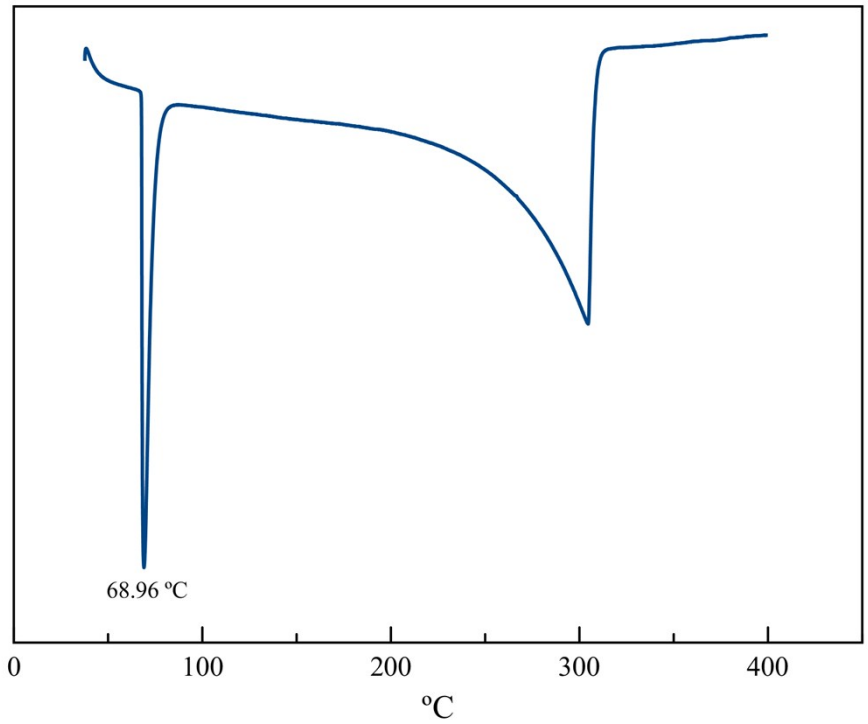

Figure S19. DSC curve of the pure **ldc** reactant.

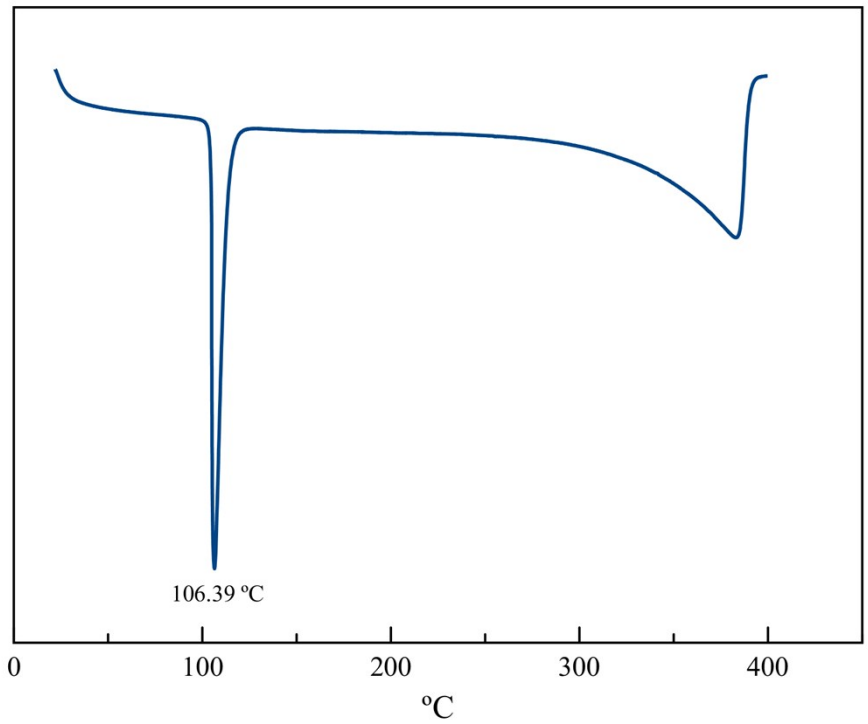

Figure S20. DSC curve of the pure **pxf** reactant.

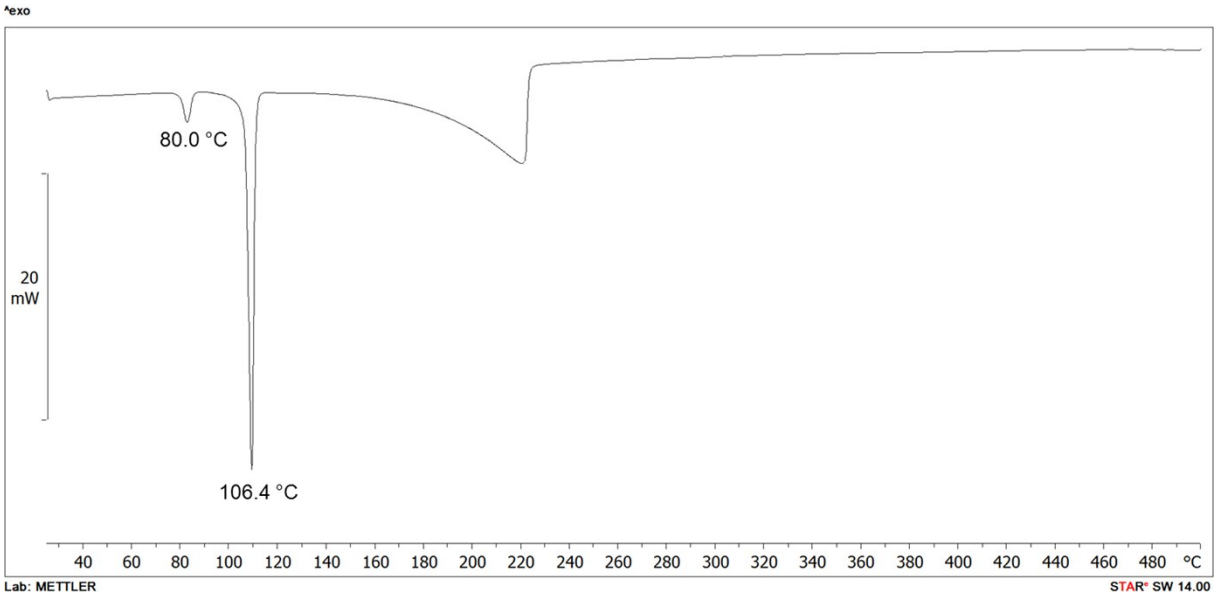

Figure S21. DSC curve of the pure **tfib** reactant.

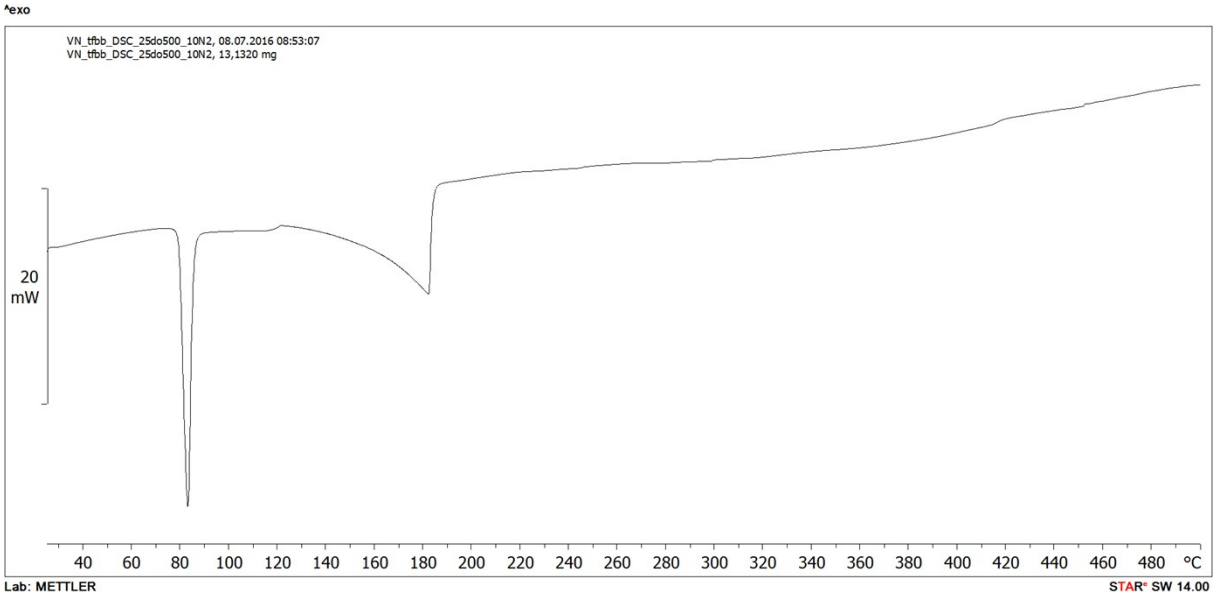

Figure S22. DSC curve of the pure **tfbb** reactant.

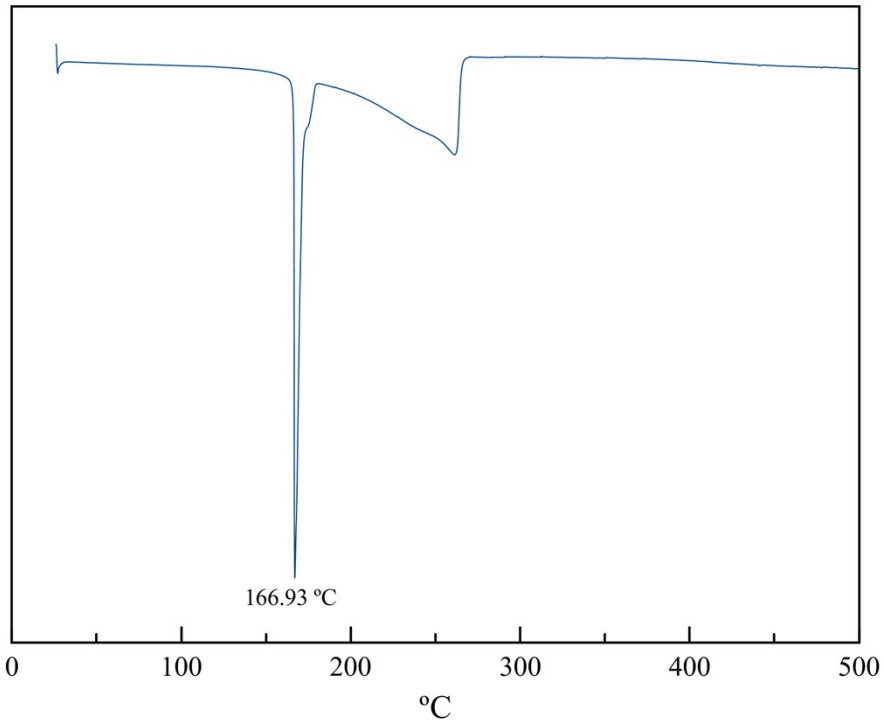

Figure S23. DSC curve of the cocrystal **(pza)$_2$(tfib)**. The sample was heated in sealed aluminium pan.

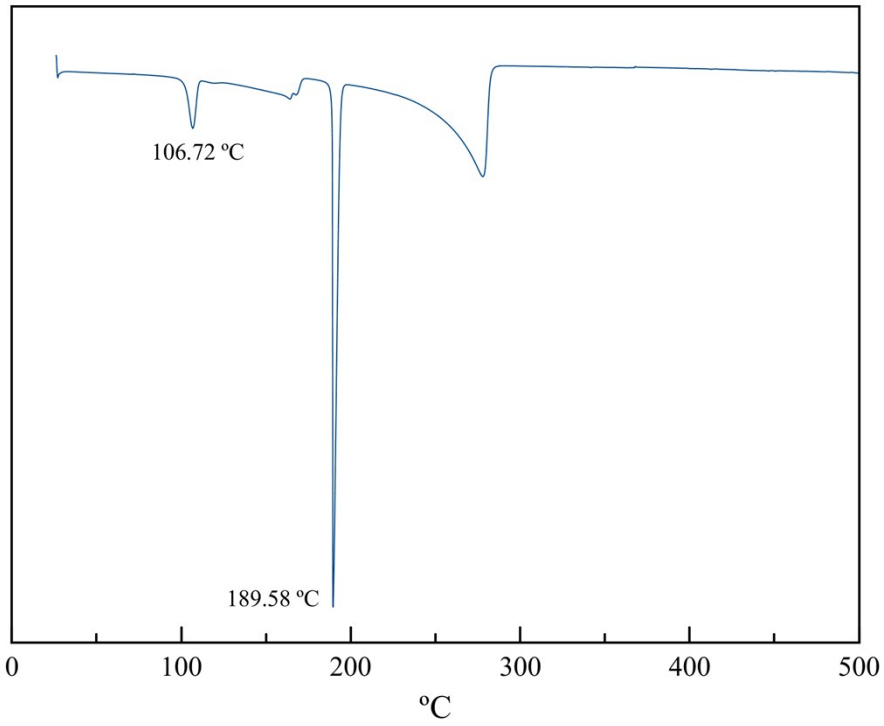

Figure S24. DSC curve of the cocrystal **(pza)$_2$(tfbb)**. The sample was heated in sealed aluminium pan.

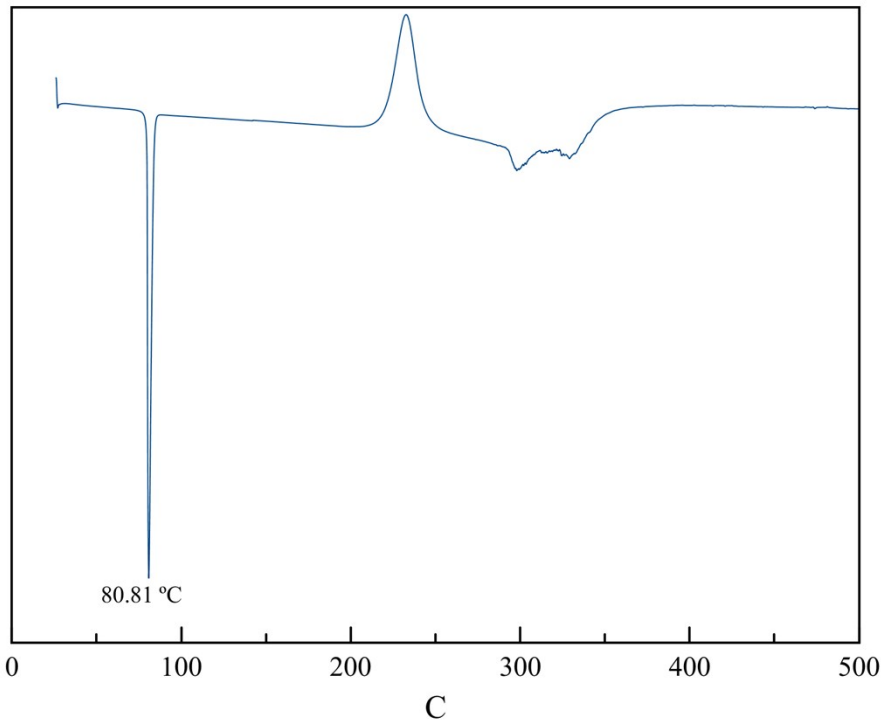

Figure S25. DSC curve of the cocrystal (**ldc**)$_2$(**tfib**). The sample was heated in sealed aluminium pan.

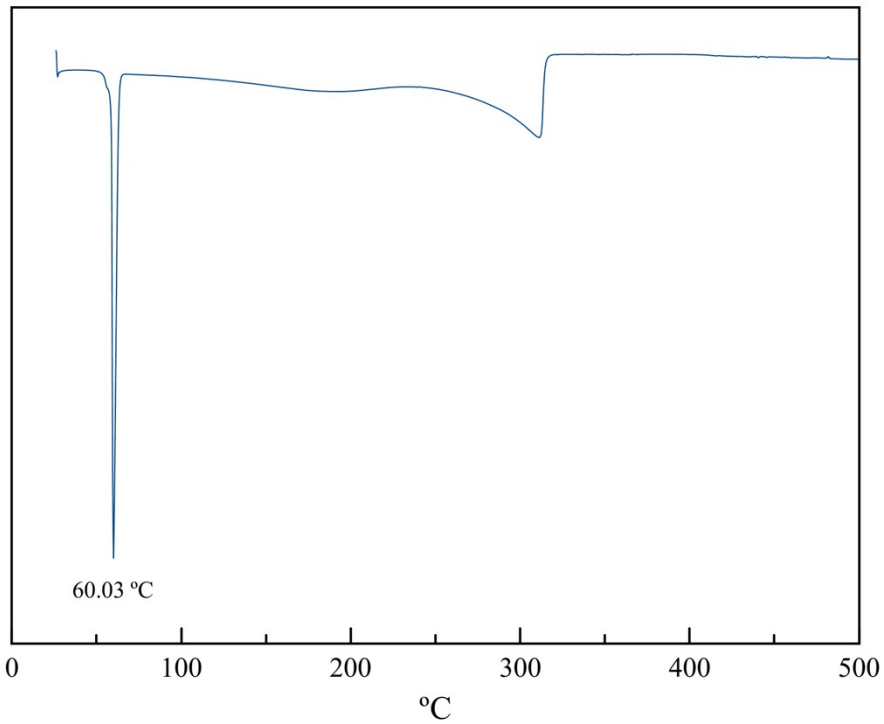

Figure S26. DSC curve of the cocrystal (**ldc**)$_2$(**tfbb**). The sample was heated in sealed aluminium pan.

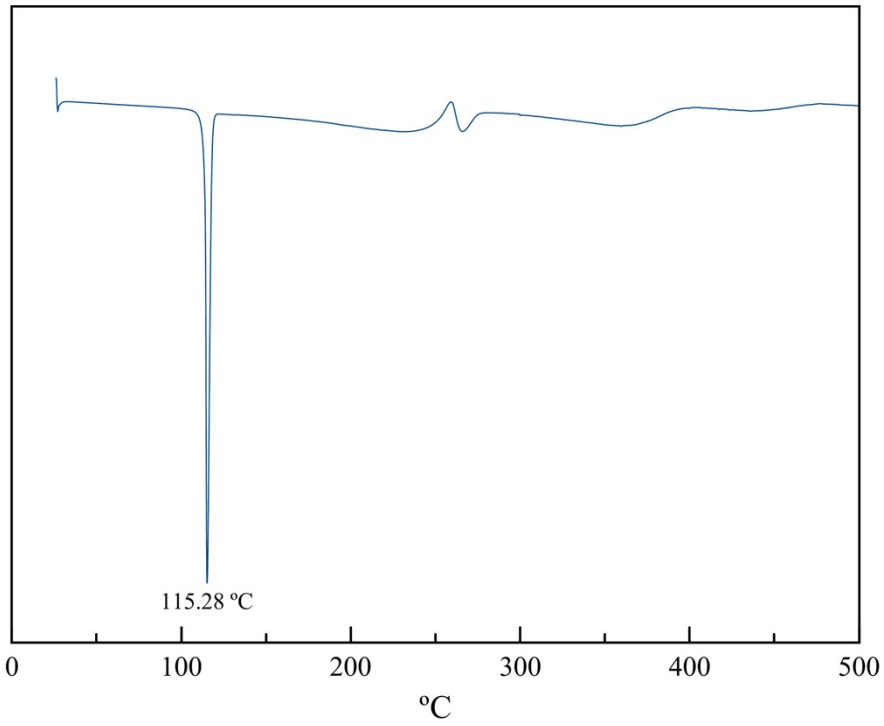

Figure S27. DSC curve of the cocrystal (**pxf**)(**tfib**). The sample was heated in sealed aluminium pan.

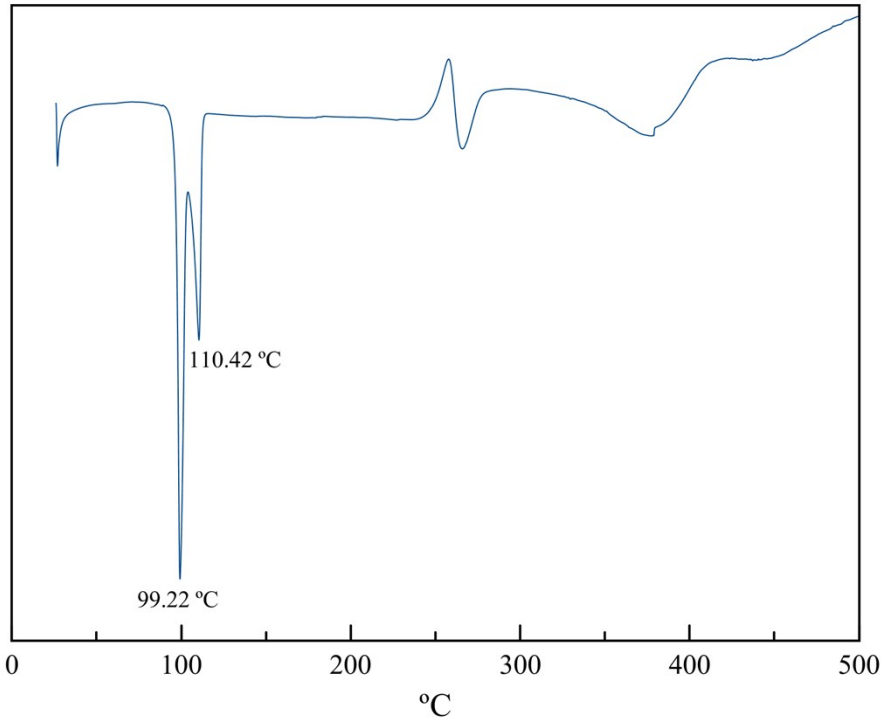

Figure S28. DSC curve of the product of grinding a mixture with a 2:1 molar ratio of **pxf** to **tfib** (a mixture of (**pxf**)(**tfib**) and **pxf**). The sample was heated in sealed aluminium pan.

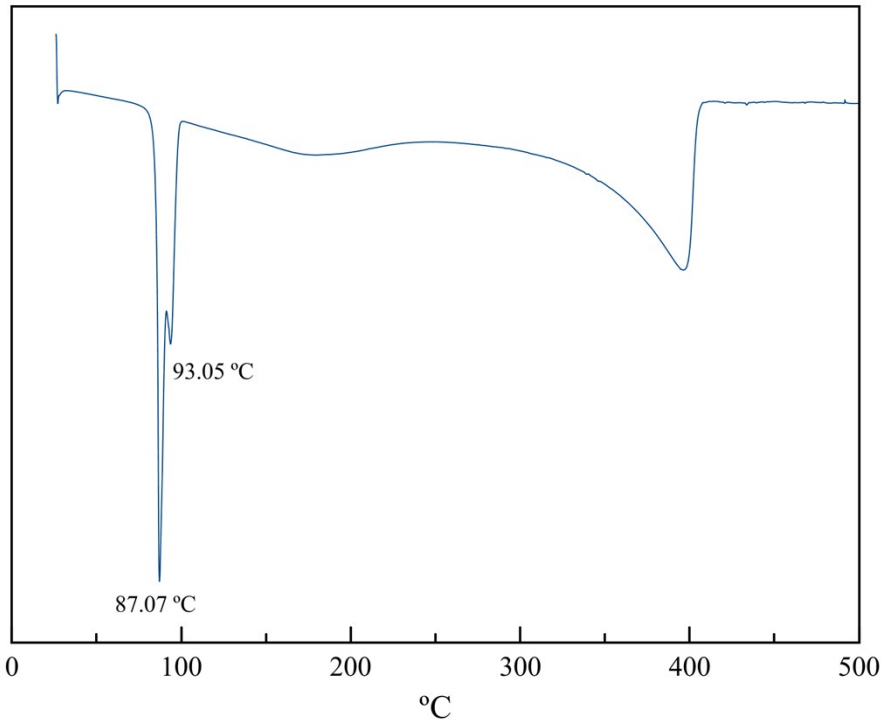

Figure S29. DSC curve of the cocrystal (**pxf**)$_2$(**tfbb**). The sample was heated in sealed aluminium pan.

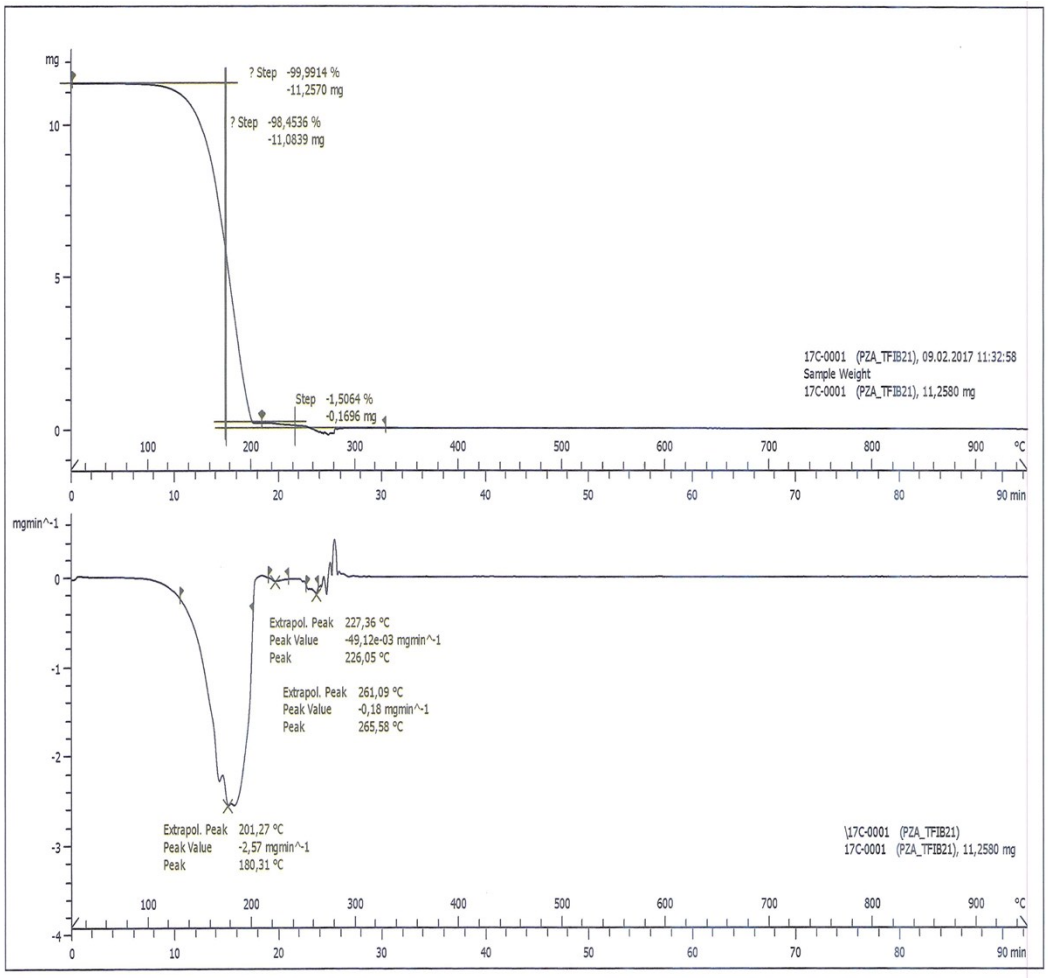

Figure S30. TG (top) and DTA (bottom) curve of the cocrystal (**pza**)$_2$(**tfib**). The sample was heated in open alumina pan.

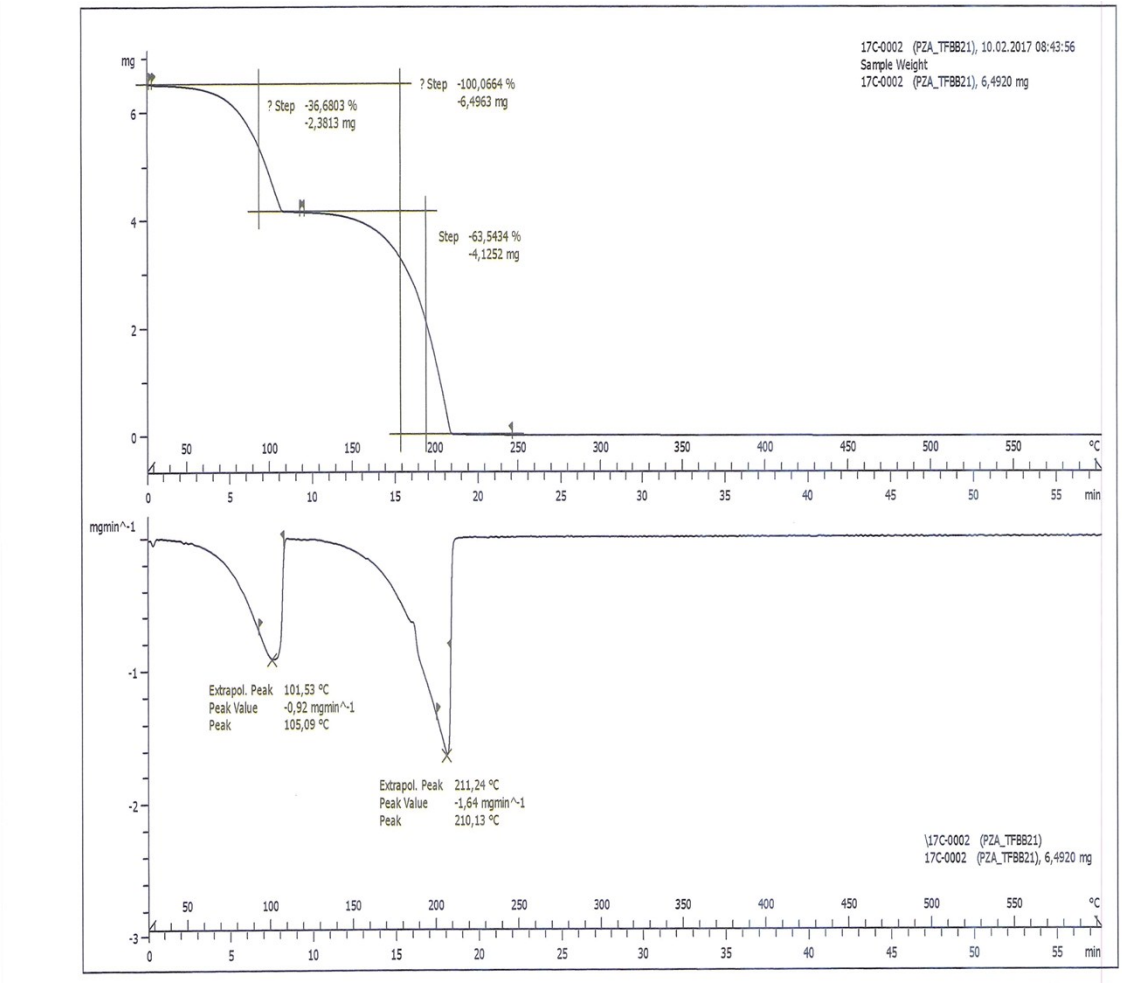

Figure S31. TG (top) and DTA (bottom) curve of the cocrystal (**pza**)$_2$(**tfbb**). The sample was heated in open alumina pan.

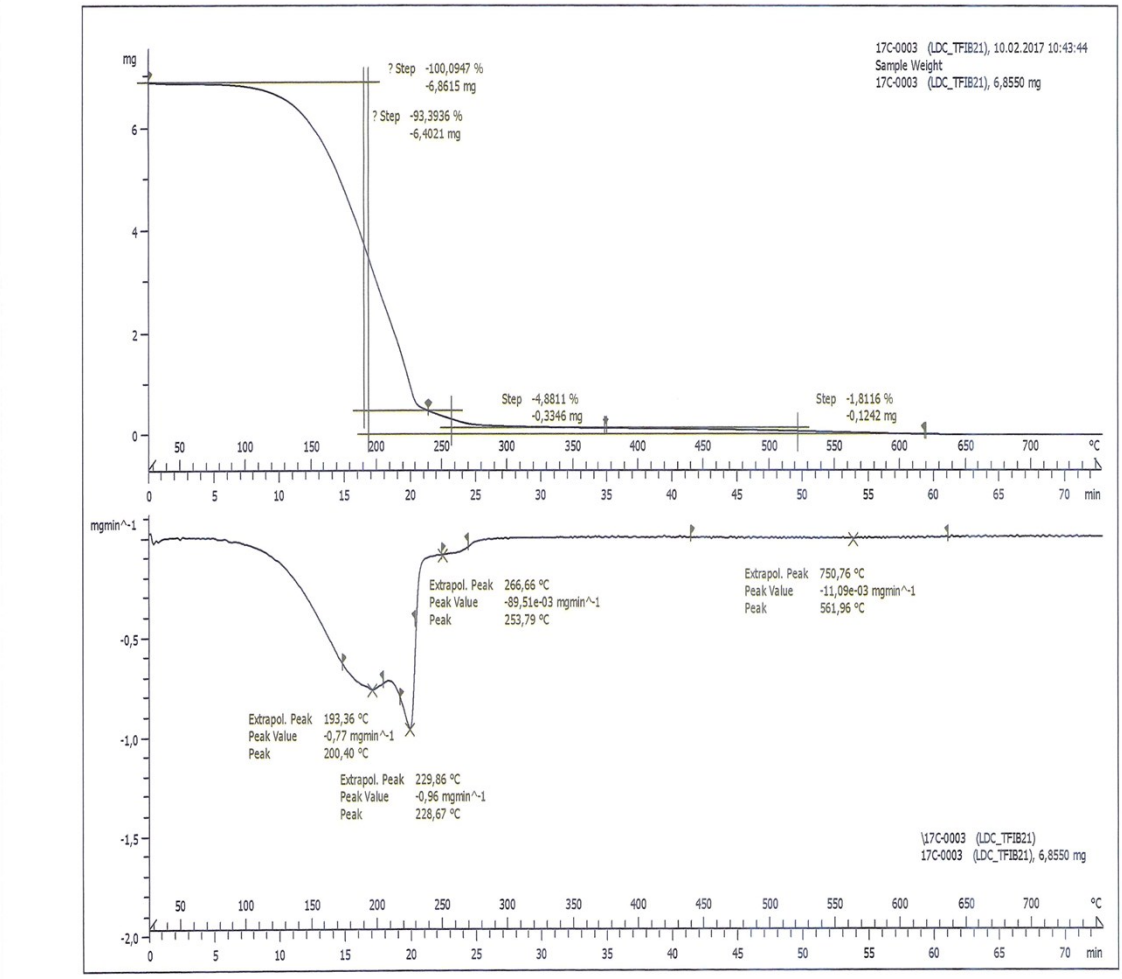

Figure S32. TG (top) and DTA (bottom) curve of the cocrystal (**ldc**)$_2$(**tfib**). The sample was heated in open alumina pan.

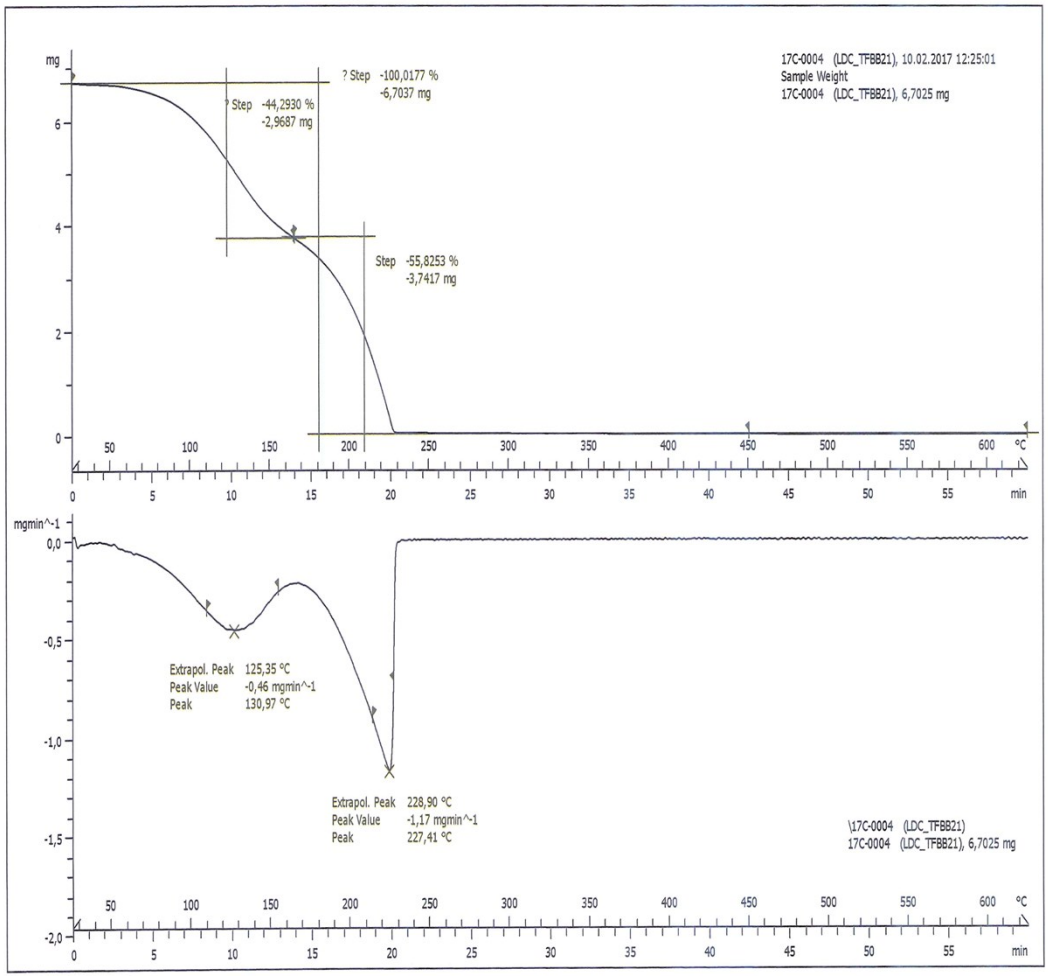

Figure S33. TG (top) and DTA (bottom) curve of the cocrystal (**ldc**)$_2$(**tfbb**). The sample was heated in open alumina pan.

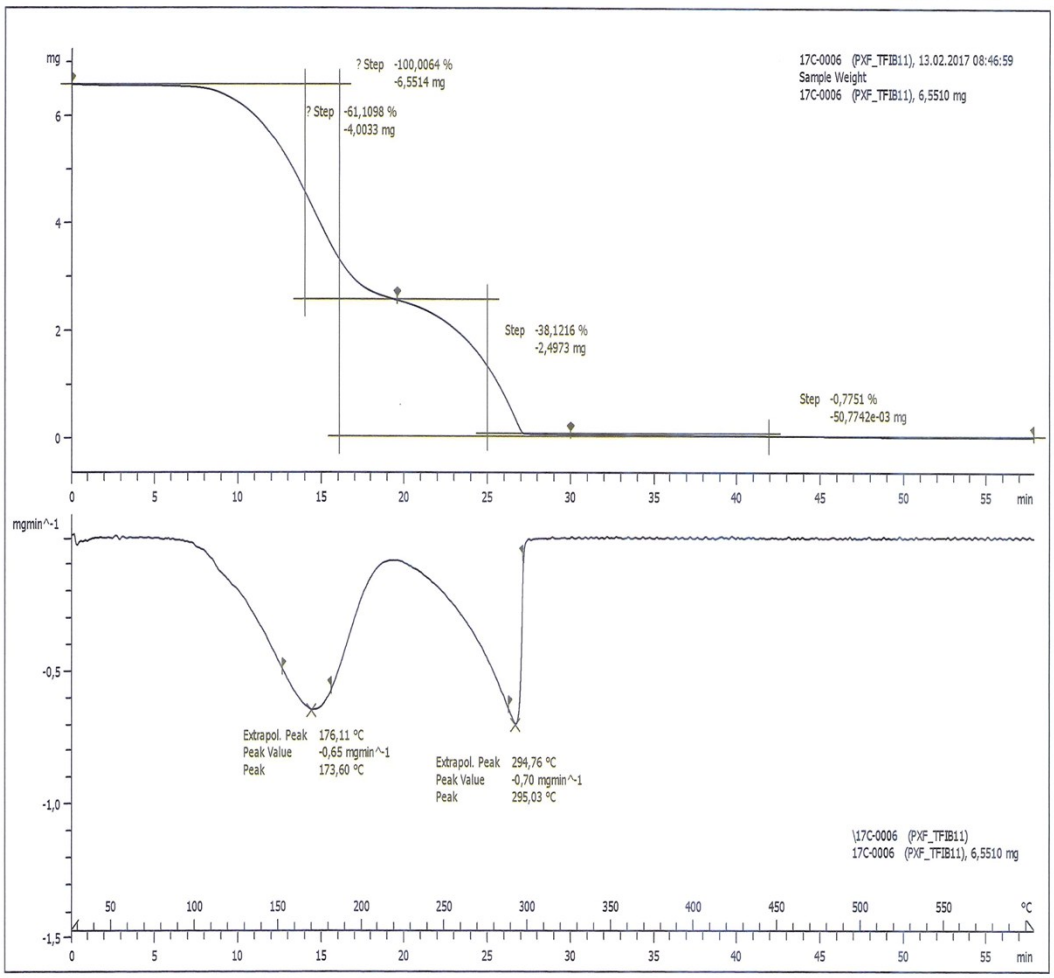

Figure S34. TG (top) and DTA (bottom) curve of the cocrystal (**pxf**)(**tfib**). The sample was heated in open alumina pan.

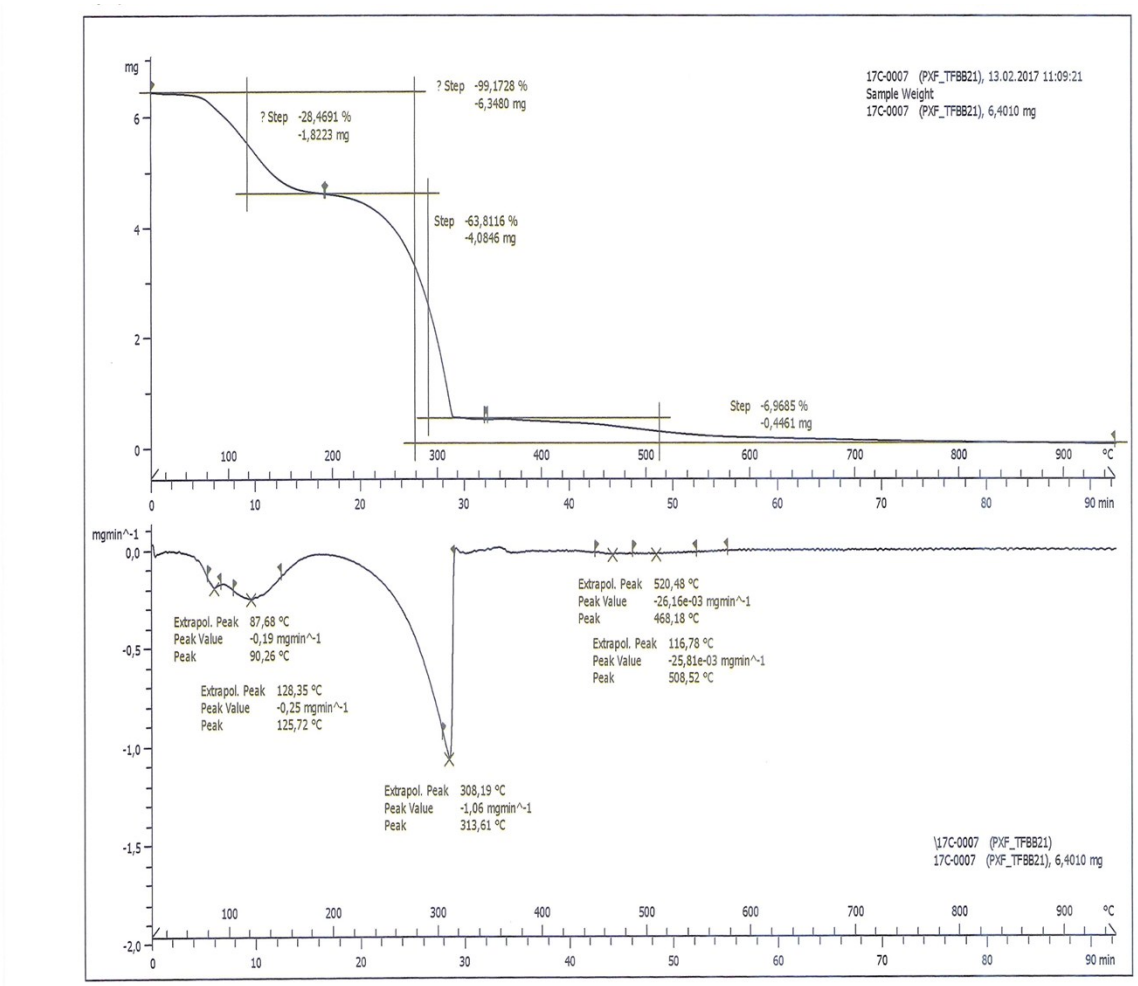

Figure S35. TG (top) and DTA (bottom) curve of the cocrystal (**pxf**)$_2$(**tfbb**). The sample was heated in open alumina pan.